scientific reports

OPEN

Optimizing oil properties and asphaltene management using Fe_3O_4-based nanohybrids under microwave radiation

Hamidreza Farshadfar, Reza Gharibshahi, Arezou Jafari & Sharif Shoushtari

Due to the depletion of heavy oil reservoirs, novel approaches such as microwave technology and the integration of nanoparticles have expanded significantly. In this study, Fe_3O_4 nanoparticles, along with Fe_3O_4-SiO_2 and Fe_3O_4-NiO nanohybrids, were synthesized via a co-precipitation method and characterized using various tests. Furthermore, to enhance the effect of the nanoparticles, MW irradiation was employed, modifying the static properties of crude oil. The optimal conditions, identified using the Taguchi design of experiment approach, revealed Fe_3O_4-NiO to be the best option at a concentration of 0.5 wt.%, with 400 watts of power under 9 min of irradiation period. Under these conditions, a 42% reduction in viscosity, a 4.47° API gravity increase attributed to the breakdown of heavy molecules like asphaltenes. Also, it was revealed that this hybridizing approach leads to the stabilization of asphaltene particles, which was assessed by measuring the onset of asphaltene precipitation. The onset, evaluated with and without MW treatment, revealed a significant shift from 10 Vol.% to 26 Vol.% of n-heptane volume under optimal conditions. Furthermore, asphaltene content in the oil sample decreased by 22.6%, and sulfur content in asphaltenes dropped by 52.6%. These investigations, along with the conducted structural analysis tests provide novel evidence supporting our hypothesis regarding the stability of asphaltene particles in the presence of nanoparticles and MW energy, a methodology that has not been previously explored in the literature.

Keywords Microwave, Nanohybrid, Viscosity, Asphaltene, Onset, Precipitation

As a significant number of oil reservoirs approach their final stages, there is an increasing demand for the production of heavy hydrocarbons through cost-effective methods. One of the most recent approaches in this regard is the use of MW, which unlike other heating methods will lead to a uniform distribution of temperature throughout the reservoir[1,2]. The use of MW, in particular, offers benefits such as uniform distribution of energy and temperature in the reservoir due to the creation of a hot zone. This will ultimately cause the heavy components of oil to break down, which is followed by the decrease of the viscosity, and an increase in °API[3]. Furthermore, MW radiations will influence the bonds of polar components of the hydrocarbons, initiating the release of sulfur compartments[4]. These waves alone have a low penetration depth and can only affect the near wellbore[5]. Also, crude oil is not a good absorber for these MW energy[6]. In order to improve the performance of MW and transfer heat to places far from the well, magnetic materials can be used to absorb the waves energy in the presence of electromagnetic field[7].

Nanoparticles are used in Enhanced Oil Recovery (EOR) to improve sweep efficiency[8], alter reservoir rock wettability, reduce capillary forces, and change interfacial tension[9], enhancing oil recovery . Some nanoparticles act as catalysts for in-situ oil upgrading, breaking down heavy crude oil into lighter components, reducing extraction and refinement costs[10]. Energy for these reactions can come from steam injection, in-situ combustion, or MW[11]. Nanoparticles address flaws in conventional EOR methods, which can be costly and operationally challenging[12]. Their benefits include a high surface-to-volume ratio for maximum interactions[13–15], small size preventing pore blockage[16], and environmental advantages[17]. Fe_3O_4 nanoparticles are commonly used in EOR studies and have been shown to reduce viscosity and upgrade heavy oil[18–21]. Silica (SiO_2) is another one of the most utilized nanoparticles in the literature in different forms. One of the most advantageous aspects of SiO_2 nanoparticles is their cost-effectiveness. Ragab et al.[22] investigated the effect of SiO_2 nanoparticles on oil recovery. The ultimate results indicated a 19% improvement oil recovery, with the main mechanism being IFT and viscosity reduction.

Faculty of Chemical Engineering, Tarbiat Modares University, Tehran, Iran. ✉email: ajafari@modares.ac.ir

A crucial discovery in recent studies is the ability of certain nanoparticles to absorb the radiated energy from MW. Absorber and dielectric nanoparticles that can either absorb MW radiation or modify its electromagnetic properties, including Fe_3O_4, nickel oxide (NiO), and activated carbon, can be utilized to enhance the effects of MW radiation beyond their in-situ upgrading characteristics[23–25]. In other words, the coupled process of MW and heavy component (asphaltene, resin, wax, etc.) absorption on the surface of nanoparticles, will cause direct exposure to the wave energy and a more effective breakdown of the heavy components, accelerating the in-situ oil upgrading process[26–28].

Utilizing nanoparticles alongside MW can yield even better results due to some nanoparticles ability to absorb it energy. Results showed that these magnetic nanohybrids are good absorbers for MW and cause a further increase in the temperature of oil exposed to MW. Also, the results of using these nanoparticles in micro model tests show a significant increase in oil recovery. By incorporating metal oxide nanoparticles into the injection fluid, more MW energy is absorbed, increasing the oil's temperature. This heightened temperature decreases both the oil's viscosity and the resistance along its path. Consequently, the injection fluid directs the oil to the production well with improved efficiency. Interruption time when MW was used was much less than nanofluid injection without MW. This is due to the absorption of MW energy through the injection fluid. Therefore, water is converted from liquid phase to vapor and with the increase in the mobility of the vapor phase, the time of injection in the porous medium is reduced[3,20,29].

One major heavy component found in crude oil is asphaltene, which can cause flow assurance issues in near wellbore, wellbore and pipelines. Solutions such as inhibitors and methods for removing deposited asphaltene from porous media was performed[30]. Due to the polarity of asphaltene particles, nanoparticles have shown promise as inhibitors for asphaltene and prevent its precipitation by creating an electrostatic balance. Additionally, if the activation energy is provided to break down asphaltene, nanoparticles can act as nanocatalysts and increase the reaction rate[14]. The simultaneous effect of nanoparticles and MW provides a uniform of heat distribution in the porous media, that cause accelerates the reaction rate of breaking down heavy crude oil component[31].

In previous studies, the improvement of oil quality in this process was assumed to be due to the breakdown of heavy molecules such as asphaltene, but the amount of asphaltene, the structure of asphaltene, and its onset of precipitation have not been thoroughly investigated to validate this purpose. In this research, application of Fe_3O_4-based nanoparticles as inhibitors of asphaltene deposition is presented. Although the use of Fe_3O_4-based nanoparticles has been employed to prevent asphaltene precipitation also utilizes MW to enhance their performance. The hypothesis is validated through the examination of SEM images, FTIR, and EDS tests. The stability of asphaltene particles in the presence of nanoparticles and MW energy is investigated by analyzing the onset of asphaltene precipitation which has not been previously explored. This study uniquely combines numerical and visual results to elucidate the mechanisms behind asphaltene stability. These findings demonstrate the potential of MW-assisted nanoparticle treatment to significantly enhance oil properties, making it a promising technique for the industry. Also this research conducted comparative studies, evaluating the performance of these novel nanoparticles against other nanoparticles under identical conditions.

Material and methods

The current study presents an efficient nanohybrid material aimed at improving the static properties of crude oil and increasing the instability of asphaltenes during the MW heating process. Optimal conditions were identified using the Taguchi approach. Subsequently, the onset of asphaltene precipitation was measured, and the asphaltenes were extracted and characterized using various methods. A schematic flow chart of the experimental procedure for this research is shown in Fig. 1.

Materials

In previous studies, it was mentioned that during calcination, Fe_2O_3 was formed instead of Fe_3O_4. Therefore, in this research, the co-precipitation method was used to synthesize of Fe_3O_4[20,32,33] and its hybrid with NiO and SiO_2. Iron (III) chloride hexahydrate ($FeCl_3{\cdot}6H_2O$), iron (II) chloride tetrahydrate ($FeCl_2{\cdot}4H_2O$), Ammonium hydroxide (NH_4OH) and deionized water (DI-water) were utilized for Fe_3O_4 synthesis with co-precipitation method. NiO and SiO_2 (10–20 nm, 11–14 nm) was supplied from US-NANO which were hybridized with Fe_3O_4. To obtain the Fe_3O_4-NiO and Fe_3O_4-SiO_2 hybrids, to prevent side-reaction and unwanted byproducts, N_2 gas was injected bubble-wise throughout the process. Oleic acid, normal heptane and alcohol were also used to surface modification of the SiO_2 nanoparticle.

The oil utilized in this study was extracted from a field in southwestern Iran. It had a density of 0.9343 g/cm^3 (19.95°API) and a viscosity of 330 centipoise (cP) at room temperature, with an asphaltene content of 11.7%.

Synthesis, surface modification and characterization of nanoparticles

Fe_3O_4-NiO and Fe_3O_4-SiO_2 were synthesized through co-precipitation method like Fe_3O_4. Initially, NiO and SiO_2 nanoparticles were dissolved in 50 ml of deionized water and sonicated for 30 min, this process transforms the nanoparticles into the primary sites for reacting with precursors in order to create Fe_3O_4nanoparticles[20]. As a result, Fe_3O_4 nanoparticles will form on the outer surfaces of NiO and SiO_2 nanoparticles. Due to high reactivity of materials at the nanoscale, these nanoparticles will become tightly bound together. To obtain a 1:1 weight ratio, 1 g of NiO and SiO_2 nanoparticles were added to a three-necked flask along with 2.335 g of $FeCl_3{\cdot}6H_2O$ and 0.858 g of $FeCl_2{\cdot}4H_2O$. Thereafter, DI-water was added to reach a solvent volume of 200 ml and the solution was stirred vigorously for 30 min. The solution was maintained in water bath (75 °C). As discussed earlier, N_2 was injected throughout the process for maximum product purity. Following the co-precipitation guidelines for the synthesis of Fe_3O_4 nanoparticle, ammonia solution was added drop wise to the mixture until its pH reaches 11. Lastly, the solution was washed with DI-water under 0.5 Tesla magnetic field and subsequently the black precipitations were placed in the oven under 60 °C for 12 h.

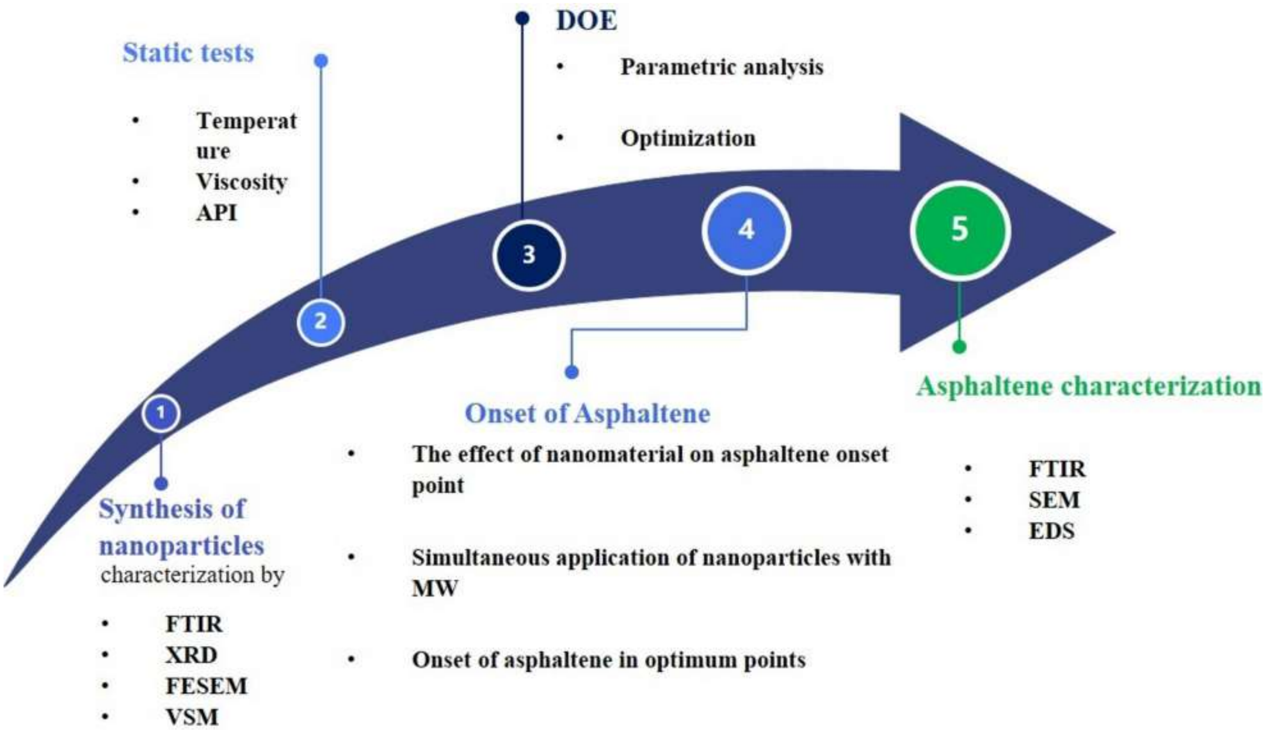

Fig. 1. Schematic flow chart of the experimental procedure.

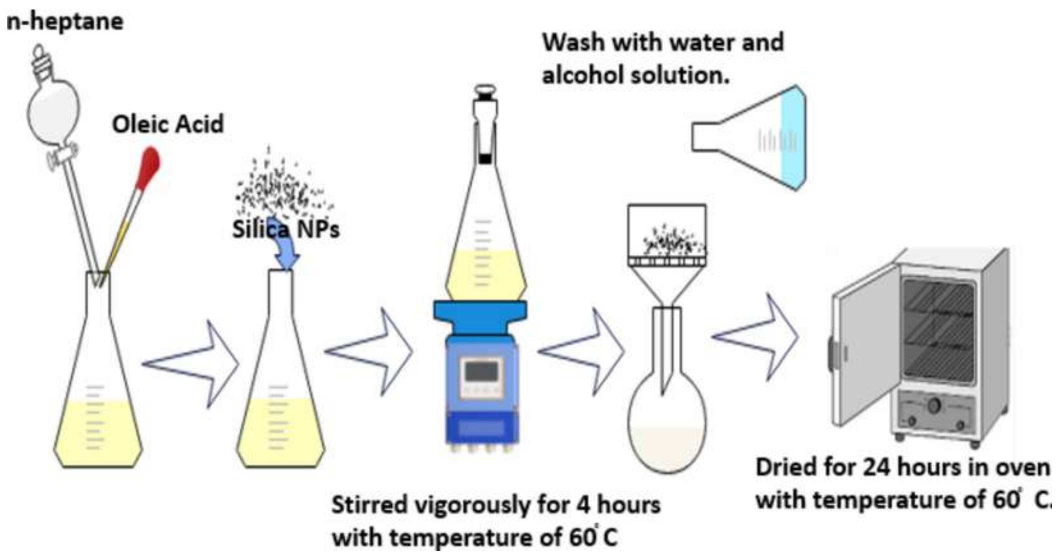

Fig. 2. Surface modification of SiO_2 nanoparticles.

Since silica is water-wet and doesn't disperse in oil, surface modification is needed to alter its wettability. As it observed in Fig. 2, this process involves mixing Oleic acid with normal heptane (1:50 volume ratio) using a magnet stirrer, and the temperature is set to 60 °C for four hours. The product is then washed using a mixture of DI-water and alcohol. After that, the white sediments are placed in the oven for 24 h (60 °C). The product, is a white oil-wet surface-modified silica and can be easily dissolved in oil[34].

After synthesis of the discussed nanoparticles, FTIR, VSM, XRD and FESEM tests were conducted to identify and measure, properties such as size, shape, composition, and the magnetic attributes. FTIR (PerkinElmer Spectrum Version 10.03.06) was conducted in powder form at room temperature to identification of the existing bonds and functional groups in synthesized nanohybrids. XRD of powderized nanoparticles was conducted on an X'Pert MPD diffractometer of the Philips Company (JEOL JDX-803) at room temperature with 30%

humidity and with Cu Ka radiation. Xray was radiated from 10 to 80 degrees with a 0.02 step size. The average crystallite size of the synthesized nanohybrids can be determined using Scherrer's equation (Eq. (1)).

$$d = \frac{K\lambda}{\beta cos\theta} \tag{1}$$

In this equation, d represents the average crystallite size of nanoparticles, K is the shape factor typically set at 0.89, β is the Full-Width Half Maximum (FWHM) indicating the peak at half of the maximum intensity, λ denotes the X-ray diffraction wavelength (λ = 0.154060 nm), and θ is the Bragg angle which is equal to 35.6°[35].

For characterization of magnetic properties of synthesized nanoparticles and nanohybrids, the VSM test was conducted (MDKB tool from Kavir Kashan Company). The samples, which were in homogeneous powder form, were placed under a magnetic field, from −10,000 Oe to 10,000 Oe, at room temperature. Other than the identification of the nanoparticle magnetic behavior type (ferromagnetic, diamagnetic, and paramagnetic), this test also measures magnetization. The shape and morphology of the synthesized nanoparticles and nanohybrid were determined using field emission scanning electron microscopy (FESEM, TESCAN 100 kx).

Temperature, viscosity and API measurement

The temperature of the crude oil and oil sample contain nanoparticles was monitored under MW radiation (2.45GHz) using an infrared thermometer (Mastech M56531C) every 30 s. The temperature of the solution acts as a gauge for the amount of MW energy being absorbed by the oil solution. As the temperature of the oil solution rises, it signifies an increase in the absorbed energy, which can enhance the catalytic reaction between the oil and nanoparticles or nanohybrids creating favorable conditions for the upgrading of heavy oil. Furthermore, tracking the temperature changes over time can offer valuable insights into the efficiency and effectiveness of the energy transfer process during the MW treatment.

API and viscosity are crucial parameters to assess the effectiveness of heavy oil upgrading. In this study, API and viscosity were measured to evaluate the oil upgrading process. Viscosity was determined using the rotary method with an Anton Paar conical/cylindrical device, employing the CC27 spindle due to the high viscosity of the oil (shear rate set at 1000 rpm). Density was measured using a pycnometer and API was calculated as Eqs. 2 and 3.

$$\rho = \frac{m}{v} \tag{2}$$

$$API = \frac{141/5}{\rho} - 131/5 \tag{3}$$

Statistical analysis and design of experiment (DOE)

For optimization of the effective parameters in the simultaneous effect of MW and nanoparticles in this research, an experiment design approach was utilized. Among the various experimental design methods, the Taguchi approach was chosen due to its advantages of requiring a low number of experiments and saving time compared to other methods. Given the high number of influential parameters in this research, the Taguchi L9 method involved 4 factors at three levels each, resulting in the design of 9 experiments using the Design Expert 7 software. Pre-test results indicated that nanoparticle type, concentration, power, and radiation time were the most critical parameters, which were then selected for further experimentation as presented in Table 1. The value of density and viscosity can show the quality of the oil. Also the temperature of oil is the parameter that show the amount of MW energy absorbed by each of oil samples. Therefore, the responses of experiment design are viscosity (cP), density (gr/cm^3), and temperature (°C).

Asphaltene onset precipitation measurement, extraction and characterization

There are multiple methods introduced in the literature for the determination of the onset point of asphaltene[36]. However, the fundamental approach is based on alteration of three parameters; pressure, temperature, and composition. The conditions under which temperature alteration causes asphaltene onset seldom happens in the reservoir. The composition approach was chosen for triggering the onset point of asphaltene based on Escobedo and Mansoori[30] method. This method entails changing the composition of the heavy crude oil, by preparing different solution with various n-heptane volume percentage (Vol. %). During this process the oil becomes less viscose until the asphaltene molecules flocculate. At this stage the asphaltene molecules aggregate and the viscosity of n-heptane oil solution increase so slight bump appears on the viscosity versus n-heptane Vol.% which signals onset of asphaltene precipitation.

For analyzing and measurement of asphaltene, in this study, the standard IP-143 method was used for asphaltene extraction[37,38]. Initially, 5 g of crude oil and 200 ml of normal heptane were mixed in a flask until

Level	Nanomaterial type	Concentration (wt. %)	Radiation duration (min)	Power (watts)
1	Fe_3O_4	0.01	3	400
2	Fe_3O_4-SiO_2	0.1	6	800
3	Fe_3O_4-NiO	0.5	9	1200

Table 1. DOE factors and their levels.

fully dispersed and then shaked for 1 h and stored in a dark cupboard for 72 h. The liquid was decanted into filter paper without agitation, followed by transferring the residue with hot heptane. The filter paper and its contents were refluxed with heptane for 1 h in a different flask. Subsequently, 100 ml of toluene was added and refluxing continued until all asphaltene was dissolved. The content was then transferred to a dry evaporating vessel to remove toluene. For characterization of extracted asphaltene, the existing bonds were identified using FTIR test. Aromatic, Aliphatic, Sulfoxide, Alkane chain, and Aliphatic/Aromatic ratio indexes were defined as Eqs. 4 through 8, for asphaltene to identify based on the FTIR test. A represents the surface area under the intensity curve plot in terms of wavelength[39–41]. The structures of the asphaltene samples were investigated and compared using SEM images. Energy dispersive X-ray spectrometry (EDX, VEGA-TESCAN-LMU) was utilized for the elemental analysis and chemical characterization of asphaltenes.

$$\text{Aromatic Index} = \frac{A_{1600}}{\sum A} \tag{4}$$

$$\text{Aliphatic} = \frac{A_{1460} + A_{1376}}{\sum A} \tag{5}$$

$$\text{Sulfoxide Index} = \frac{A_{1030}}{\sum A} \tag{6}$$

$$\text{Alkane chane Index} = \frac{A_{724}}{A_{1460} + A_{1376}} \tag{7}$$

$$\sum A = A_{724} + A_{743} + A_{814} + A_{864} + A_{1030} + A_{1376} + A_{1460} + A_{1600} + A_{1700} + A_{2862} + A_{2923} + A_{2953} \tag{8}$$

Result and discussion

Nanoparticle characterization

The functionalization was confirmed using FTIR spectroscopy to ensure the characterization of the synthesized nanohybrids. FTIR of the surface-modified SiO_2 is shown in the Fig. 3. As is observed, the peaks at wavelengths of 468, 812, 1111, and 979 cm^{-1}belong to the rocking vibration, symmetric stretching vibration, asymmetric stretching vibration of O-Si–O, and Si–OH bonds[42] respectively. The peak observed at 1463 cm^{-1}[43] was assigned to the scissoring vibration of C-H bonds .The 1573 and 1713 cm^{-1}peaks[43] are carboxylate group on the surface of silica nanoparticle formed by reaction showed in Eq. 9, and the bonds 2855, and 2926 cm^{-1}[42] show that long alkyl chains, which exists on structure oleic acid. Consequently it can be concluded that the surface modification of silica nanoparticle with oleic acid was successful, indicating that the surface of the silica nanoparticles is now oil-wet and can maintain the heavy components of the heavy oil, specifally asphaltene.

$$\mathrm{SiO_2(OH)}_n + \mathrm{yHOOCC_{17}H_{33}} \rightarrow \mathrm{SiO_2(OH)}_{n-y}(\mathrm{OOCC_{17}H_{33}})_y + \mathrm{yH_2O} \tag{9}$$

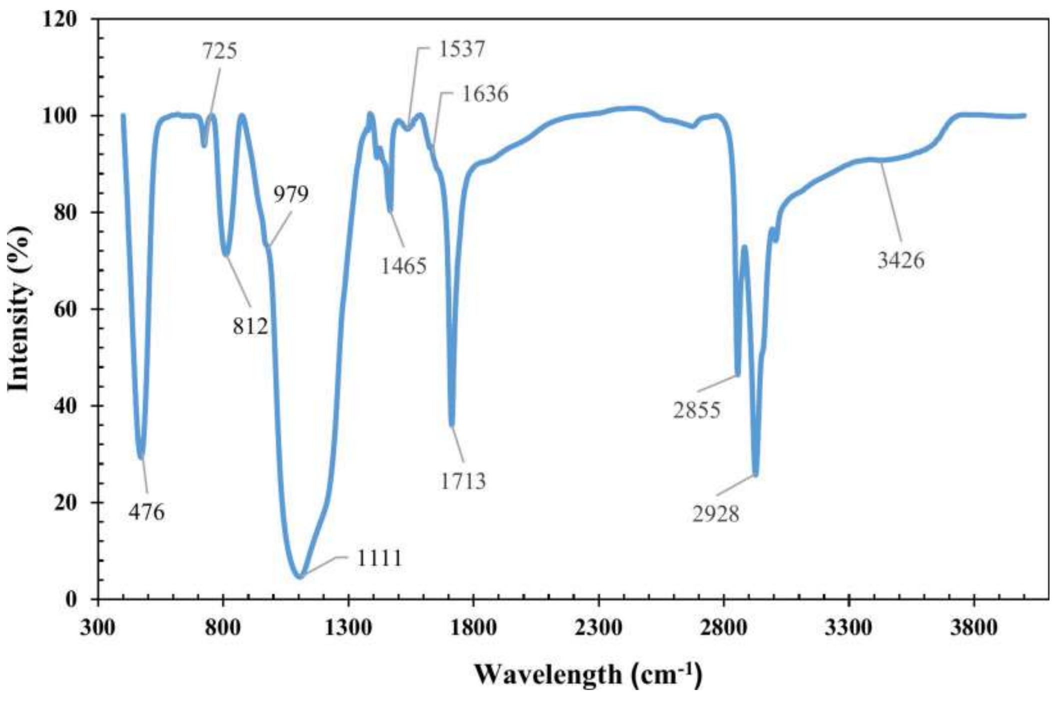

Fig. 3. FTIR results for the surface modified silica nanoparticles.

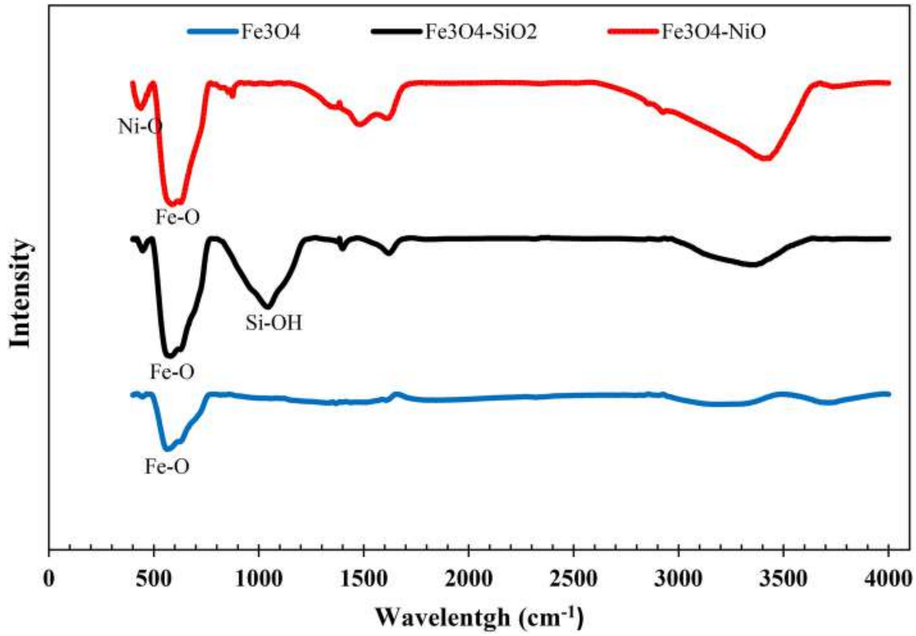

Fig. 4. FTIR results for Fe_3O_4, Fe_3O_4-SiO_2, and Fe_3O_4-NiO nanomaterials.

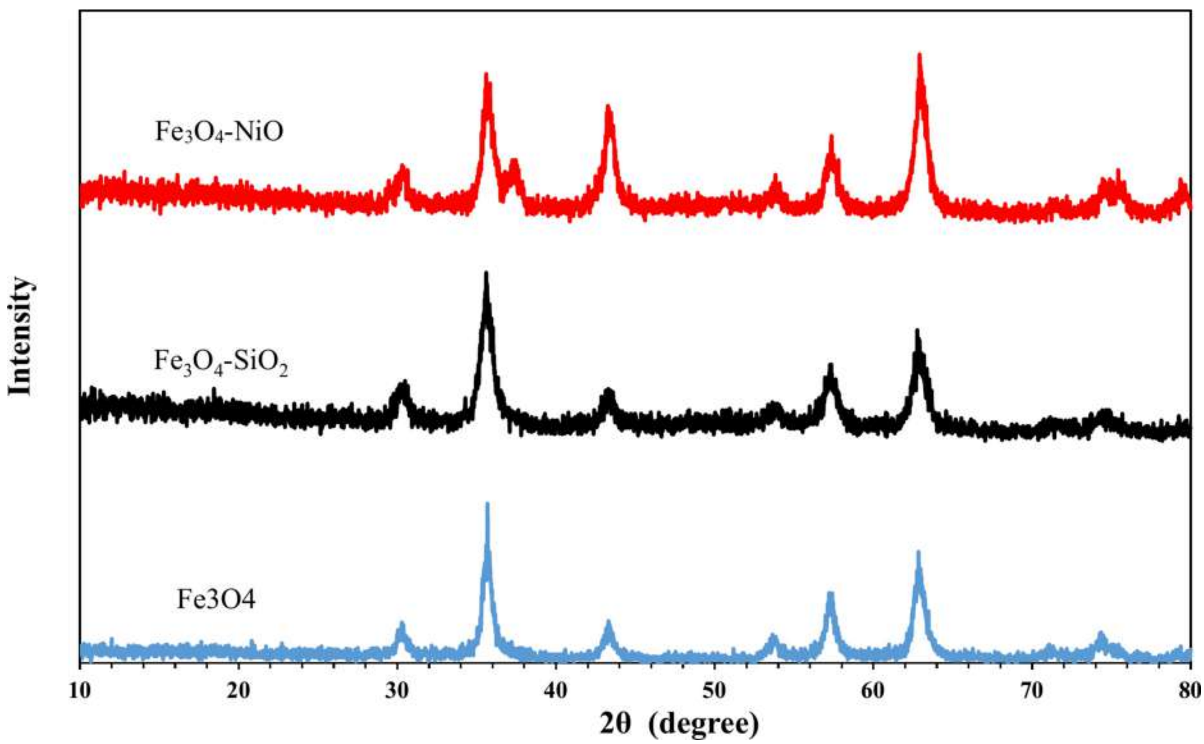

Fig. 5. The XRD results for Fe_3O_4, Fe_3O_4-SiO_2, and Fe_3O_4-NiO nanomatrials.

As shown in Fig. 4 the 566 cm^{-1}peak in the FTIR spectroscopy illustrates the Fe–O bond peak in all of the synthesized nanoparticles[20]. For Fe_3O_4-SiO_2 nanohybrid the rocking vibration O-Si–O asymmetric O-Si–O, and Si–OH bonds are shown in 456, 1104 and 1052 cm^{-1} peaks. Also the Ni–O bonds were recognized by the 443 and 636 cm^{-1} peaks. Also, the peaks at 3440 and 1400, 1624 cm^{-1}[35] is because of stretching and bending vibrations of OH group absorbed on nanohybrid surface from the surrounding when FTIR analysis was carried out.

XRD analysis was conducted to determine the crystal size and confirm the structure of the synthesized nanohybrids. The standard peaks of Fe_3O_4, Fe_3O_4-SiO_2, and Fe_3O_4-NiO are shown in Fig. 5. The XRD spectra of Fe_3O_4 and Fe_3O_4-SiO_2 are almost aligned, and the only difference between them is in related to amorphous peak at 2θ = 22°. Also, the 7.2, 43.3, 62.9, 75.4, and 79.4 peaks correspond to Ni–O bond. The existence of 43.3 and 62.9 peaks indicates that the synthesis of the Fe_3O_4-NiO was successful. Applying Scherrer's equation (Eq. 1) reveals that the average crystallite size of the synthesized Fe_3O_4 Fe_3O_4-SiO_2, Fe_3O_4-NiO nanohybrids are 14, 10, and 12 nm respectively.

Figure 6 shows the FESEM images with a 100 kx enlargement scale of Fe_3O_4, Fe_3O_4-SiO_2, and Fe_3O_4-NiO. The morphology and size of the synthesis products were characterized by FESEM. Since the Fe_3O_4 nanoparticles are spherical, the three common nanoparticles form hierarchical microspheres. The relative distribution of NiO and SiO_2 nanoparticles on the surface of Fe_3O_4 can be observed in Fig. 6b and 6c. Based on Fig. 6, the average sizes of Fe_3O_4, Fe_3O_4-NiO, and Fe_3O_4-SiO_2 nanoparticles are calculated to be 45 nm, 51 nm, and 48 nm, respectively. The conducted tests up to this point, namely, FTIR, XRD and FESEM, have fully confirmed that the intended nanoparticles have been correctly synthesized using the co-preciptation method.

In this research, the VSM analysis was performed to investigate the magnetization properties of Fe_3O_4 nanoparticles, Fe_3O_4-NiO, and Fe_3O_4-SiO_2 nanohybrids as a function of the external magnetic field. The results of the VSM analysis of the powder nanomaterials at room temperature and an applied field of – 10,000 to 10,000 Oe are depicted in Fig. 7. The S-shaped VSM results indicated that all coated and uncoated nanohybrids exhibited superparamagnetic behavior. Surface modification of the nanohybrids led to a reduction in the saturation magnetization of Fe_3O_4 from 53.76 to 43.66 and 35.46 emu/g for Fe_3O_4-NiO and Fe_3O_4-SiO_2 nanohybrids, respectively. The decrease in saturation magnetization varied depending on the type of nanoparticle hybridized with Fe_3O_4. Additionally, the coercivity (which is a measure of the magnetic hardness or resistance to demagnetization) of Fe_3O_4 nanoparticles increased upon modification with NiO and SiO_2, respectively. It must be noted that while Fe_3O_4 is capable of stabilizng asphaltenes according to the literature, NiO and SiO_2 are significantly more capable in this regard. On the other hand, NiO and SiO_2 are incapable of absorbing MW

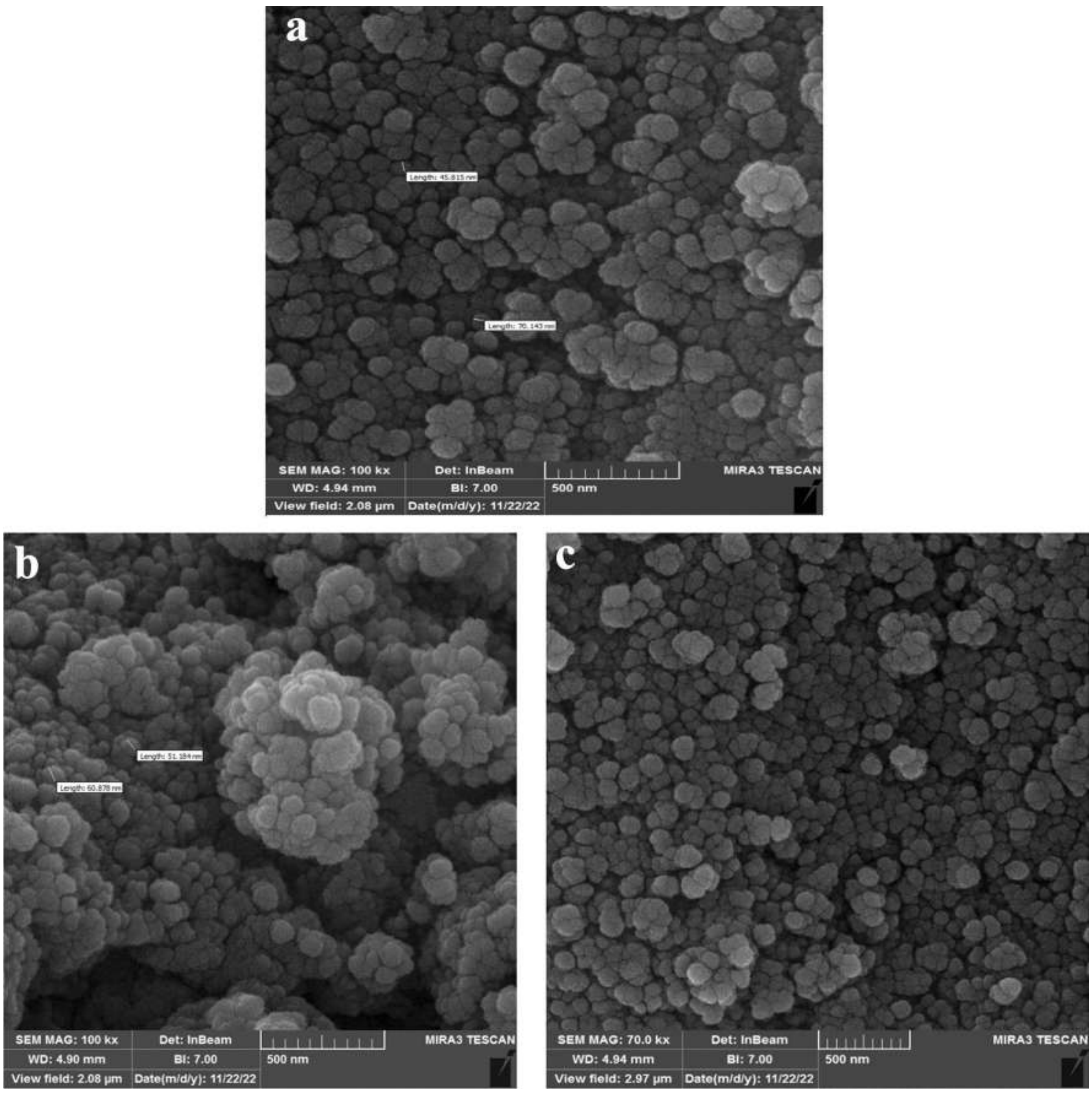

Fig. 6. FESEM images of a) Fe_3O_4 b) Fe_3O_4-NiO and c) Fe_3O_4-SiO_2 nanomaterials.

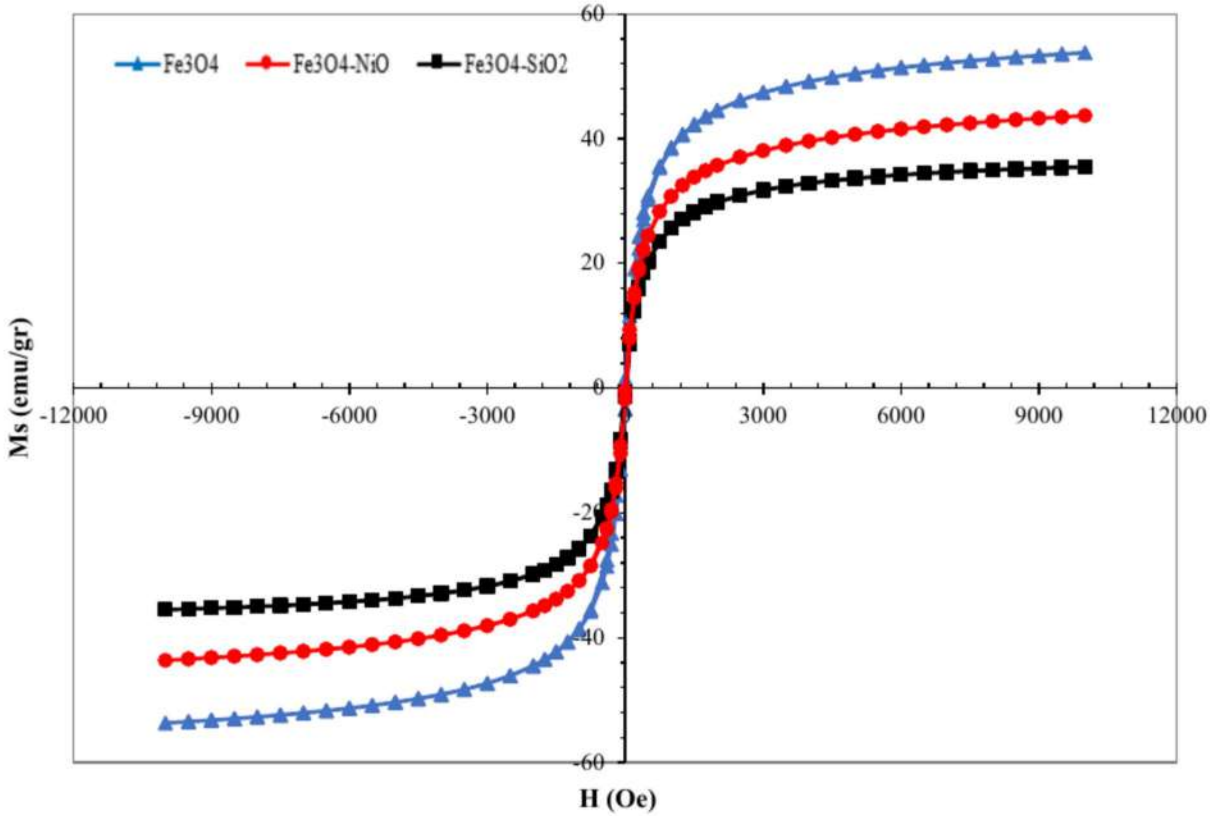

Fig. 7. VSM analysis of the synthesized Fe_3O_4, Fe_3O_4-SiO_2, and Fe_3O_4-NiO.

energy at the level of Fe_3O_4. As is observed, the hybrids of NiO and SiO_2 with Fe_3O_4, have signficantly enhanced magnetic properties. As such, the product is now expected to both stabilize asphaltene and absorb enough microwave energy to establish hotspots in the crude oil for viscosity decrease and API increase, a coupled effect that would signficantly improve recovery.

Crude oil temperature alteration in presence of nanoparticles and MW

The MW heating occurs when electric fields interact with charged particles in a material. These particles move within the material until opposing forces balance the electric force. High frequency MW create collisions between molecules, which generates heat through induced dipole moments[44]. Therefore, the solution's temperature increases through the dipole moment and hotspots generation mechanisms[6]. As a result, it can be inferred that the temperature of the oil solution serves as a reliable indicator of the energy absorbed by the oil.

The energy absorption increases upon the addition of a nanoparticles (SiO_2, NiO, Fe_3O_4, Fe_3O_4- NiO and Fe_3O_4-SiO_2), leading to an enhanced temperature surge throughout the solution. The addition of metal oxide nanoparticles increases the solution temperature[20] by increasing heat absorption due to high thermal conductivity, effective interaction with MW energy absorption. It is worth mentioning that parameters such as the concentration of the nanoparticles, power and duration of the radiation of the MW can also influence the temperature rise. To investigate the effect of nanoparticles on the temperature rise, the mentioned nanoparticles were added to the oil (0.1 wt. %) at room temperature. Initially, the aim was to analyze the influence of simultaneous MW radiation and nanoparticles. Also, during this analyses, the effect of duration and power also become obvious. All of the added nanoparticles elevated the heat absorption of the nanoparticles leading to an increase in temperature surge compared crude oil. Fig. 8 demonstrate the effects of all mentioned nanoparticles on the temperature increase of oil under 400, 800, and 1200 watts power. As is observed, all of the added nanoparticles have a positive impact on wave energy absorption. Furthermore, the effect of duration and power can be expressed by the detention of energy ($E = P.t$), indicating that the radiation duration and power both elevate the heating absorption of the oil. This is due to the dielectric properties of the nanoparticles.

Judging by Fig. 8-d, it can be concluded that Fe_3O_4-NiO has the most prominent effect on the temperature rise of the oil, followed by Fe_3O_4, Fe_3O_4-SiO_2, NiO, and SiO_2. For the 800 and 1200 watts case analyses, the trend remains the same except for Fe_3O_4-SiO_2 and NiO which switch places. As mentioned, the VSM results demonstrated that this is attributed to the Fe_3O_4-NiO nanohybrida high magnetic properties and its ability to strongly absorb MW energy. Both Fe_3O_4 and NiO have a high capacity for MW energy absorption compared to SiO_2, which is why their hybrid displays the highest temperature increase. Because SiO_2 nanoparticles have minimal magnetic properties, their MW energy absorption is lower compared to Fe_3O_4 and NiO nanoparticles. Consequently, as demonstrated by the VSM results, the energy absorption and temperature increase in the

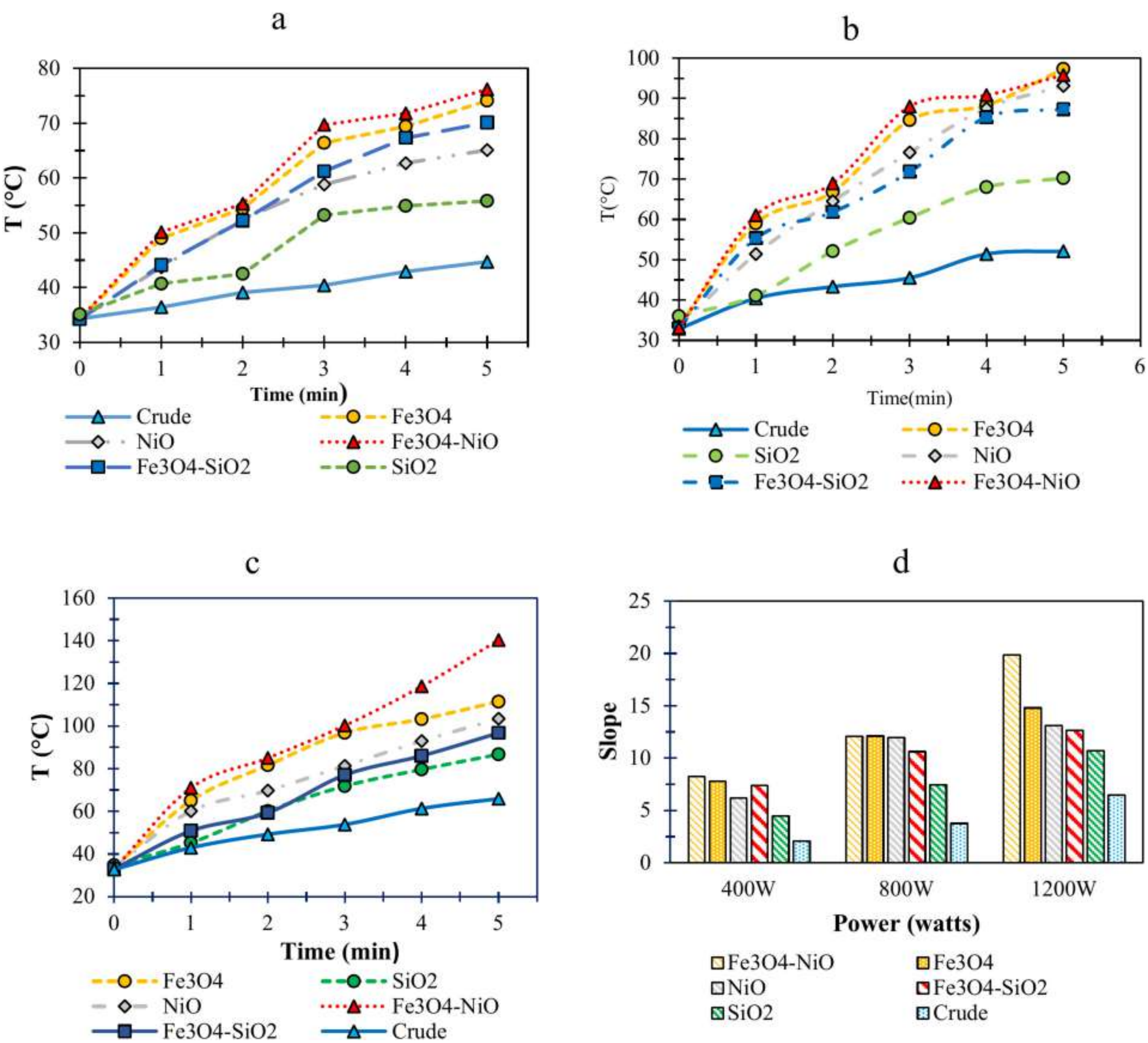

Fig. 8. a) The coupled effect of nanoparticles and hybrids with MW at 400 b) 800 c) 1200 watts d) the overall effect of increased MW radiation power on nanoparticles and nanohybrids.

Fe_3O_4-SiO_2 nanohybrid are lower than those in the Fe_3O_4-NiO nanohybrid. The temperature increase observed in Fe_3O_4-NiO nanoparticles is greater than what has been reported in the existing literature[3,45].

DOE results

The experiments were designed using the Taguchi L9 method and performed using the Design Expert 7 software. The results are shown in Table 2. In the analysis, the focus was on increasing the API degree, reducing viscosity and increasing.

In analyzing data, analysis of variance ANOVA is a useful method to identify key factors that influence the response. It involves breaking down total variance into components to assess the impact of each factor. F-values indicates greater importance and effectiveness of that parameter[3]. The analysis shows that the time of radiation of MW and concentration of nanoparticles have the most impact on reducing crude oil viscosity and increasing API degree. Additionally, MW power and time are key factors influencing the temperature of the crude oil-nanoparticle mixture. The P-value indicates the probability that the observed effects are due to random chance rather than a real relationship or effect. A low p-value (typically less than 0.05) show that the results are statistically significant. As shown in Tables 3–5 the P-values are less than 0.05 for all models, indicating their significance.

Effect of power and time parameters on responses

The effect of power of MW radiation on the viscosity, API, and temperature of crude oil is investigated in this section as shown in Fig. 9. Increasing power is considered an undesirable factor for improving the quality of crude oil. As discussed in the ANOVA results, the power and radiation time are important parameters in this process. Increasing the power causes more energy to be transferred to the oil sample, which leads to a very high

Nanomaterial type	Concentration (wt. %)	Power (watts)	Radiation duration (min)	Viscosity (cP)	API	Temperature (°C)
Fe_3O_4	0.01	400	3	275	18.24	44.6
Fe_3O_4	0.5	1200	9	210	20.81	157.1
Fe_3O_4	0.1	800	6	245	19.35	86.5
Fe_3O_4-SiO_2	0.5	400	6	235	19.84	45.6
Fe_3O_4-SiO_2	0.1	1200	3	295	17.60	67.6
Fe_3O_4-SiO_2	0.01	800	9	254	19.03	114.8
Fe_3O_4-NiO	0.01	1200	6	252	19.19	147.8
Fe_3O_4-NiO	0.5	800	3	118	20.00	59.3
Fe_3O_4-NiO	0.1	400	9	215	20.49	66.2

Table 2. The designed tests and their corresponding responses for MW radiation.

Source	Sum of squares	DOF	Mean square	F-value	p-value
Model	4685.53	5	937.11	12.37	0.0324
Type of NPs	1354.89	2	677.44	8.94	0.0545
Concentration	1276.47	1	1276.47	16.84	0.0262
Power	486	1	486	6.41	0.0852
Time	1568.17	1	1568.17	20.69	0.0199
Residual	227.36	3	75.79		

Table 3. ANOVA results of viscosity response.

Source	Sum of squares	DOF	Mean square	F-value	p-value
Model	13,064.48	4	3266.12	9.31	0.0264
Type of NPs	655.35	2	327.67	0.9345	0.4645
Concentration	48.07	1	48.07	0.1065	0.7656
Power	7783.2	1	7783.2	22.2	0.0092
Time	4625.93	1	4625.93	13.19	0.0221
Residual	1402.58	4	350.64		

Table 4. ANOVA results of temperature response.

Source	Sum of squares	DOF	Mean square	F-value	p-value
Model	6.26	5	1.25	12.32	0.0326
Type of NPs	1.81	2	0.9031	8.88	0.0549
Concentration	1.78	1	1.78	17.47	0.025
Power	0.6183	1	0.6183	6.08	0.0904
Time	2.06	1	2.06	20.27	0.0205
Residual	0.3051	3	0.1017		

Table 5. ANOVA results of API response.

temperature increase in the oil. As a result, this increase in temperature causes more light molecules to escape from the oil. However, if the power is too high, this process can also increase the viscosity and decrease the API of the oil. As can be seen in Fig. 10, with increasing time, the viscosity decreases and the API gravity increases. Therefore, it can be said that low power levels and high radiation times are suitable for optimizing the viscosity, as the energy is gradually transferred to the oil and affects its heavier molecular components. On the other hand, simultaneously increasing the power and time results in more energy being transferred to the oil, leading to a significant increase in its temperature. Based on the results shown in Fig. 9 and Fig. 10, the radiation time appears to be the most influential parameter in this process. It is important to note that in these graphs, other parameters are maintained at their optimal levels.

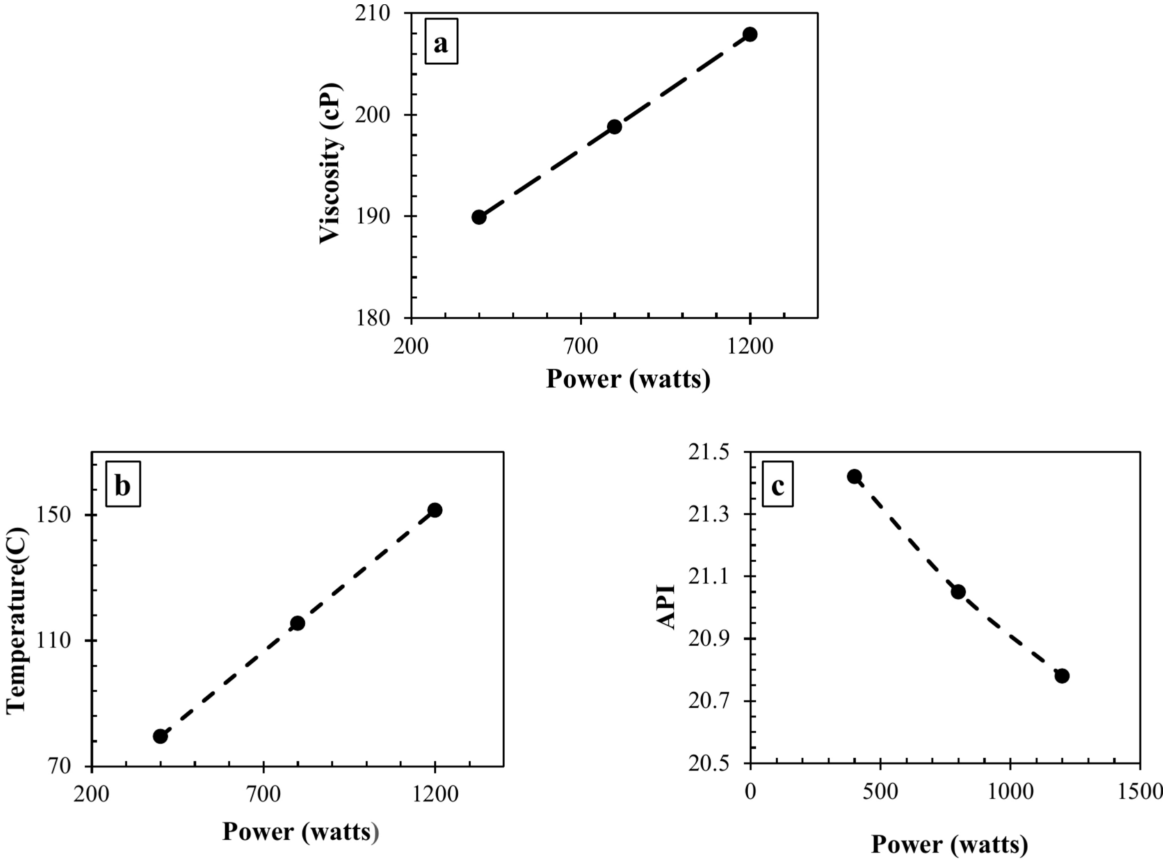

Fig. 9. Effect of power of MW on a) viscosity, b) temperature and c) API for the Fe_3O_4-NiO nanoparticle in 0.5 wt.% concentration and MW duration time of 9 min.

Interaction between nanoparticle type and concentration
Figure 11 illustrates the impact of nanoparticle type and concentration on crude oil viscosity, °API, and temperature under MW radiation exposure. According to the VSM results in section "Nanoparticle characterization", all synthesized nanoparticles possess electromagnetic properties, aligning in the electromagnetic field (MW radiation) due to their effective dispersion in oil. This alignment enhances hot spot creation performance uniformly, thereby uniformly increasing oil temperature. Due to the high electromagnetic properties of Fe_3O_4, this nanoparticle causes a greater increase in the temperature of the oil compared to Fe_3O_4-NiO and Fe_3O_4-SiO_2 nanoparticles. Additionally, the nanoparticles establish an electrostatic balance with asphaltene molecules, using absorbed energy to activate asphaltene molecule breakdown into lighter components, thereby decreasing viscosity and improving oil quality (increasing API). Because of its higher catalytic activity, Fe_3O_4-NiO nanoparticles reduce the viscosity more than Fe_3O_4 and Fe_3O_4-SiO_2.

According to Fig. 11, increasing the concentration of nanoparticles leads to enhanced MW energy absorption, resulting in an increase in internal energy by creating more hot zones within the oil solution. This increase in temperature subsequently reduces the viscosity and increases the API of the crude oil. This indicates that the 0.5 wt.% of nanoparticles is more effective compared to the other two levels (0.01 wt.% and 0.1 wt.%). The high concentration of nanoparticles causes more of them to surround the asphaltene molecules, establishing a greater repulsive force between the asphaltene and the nanoparticles. However, at very high concentrations, these forces can act in the opposite way, leading to the precipitation of the asphaltene and the nanoparticle.

Optimization

Based on the results of the experimental design, optimal points for the MW were applied to the Fe_3O_4-NiO nanoparticles at a concentration of 0.5 wt.%, 400 watts power, 9 min. For validation of the proposed optimum point for each nanoparticle (nanohybrid) and their laboratory reported viscosity, temperature and API were compared with DOE results. Table 6 shows the predicted values and the measured values of optimum point in the laboratory for viscosity, temperature, and API. The difference between these two values is generally less than 5%. Also, the results of this table demonstrates that the performance of the Fe_3O_4-NiO hybrid nanoparticles has the greatest impact on reducing crude oil viscosity and increase API in presence of MW.

Overall, the experimental results show that the use of Fe_3O_4-NiO nanohybrid with MW can be an effective and efficient method for improving crude oil quality and reducing its viscosity and increase API. In this method, the best results are obtained by increasing the time and reducing the power for MW. Moreover, Fe_3O_4-NiO nanoparticles have higher magnetic power than other nanoparticles, making them effective absorbers of

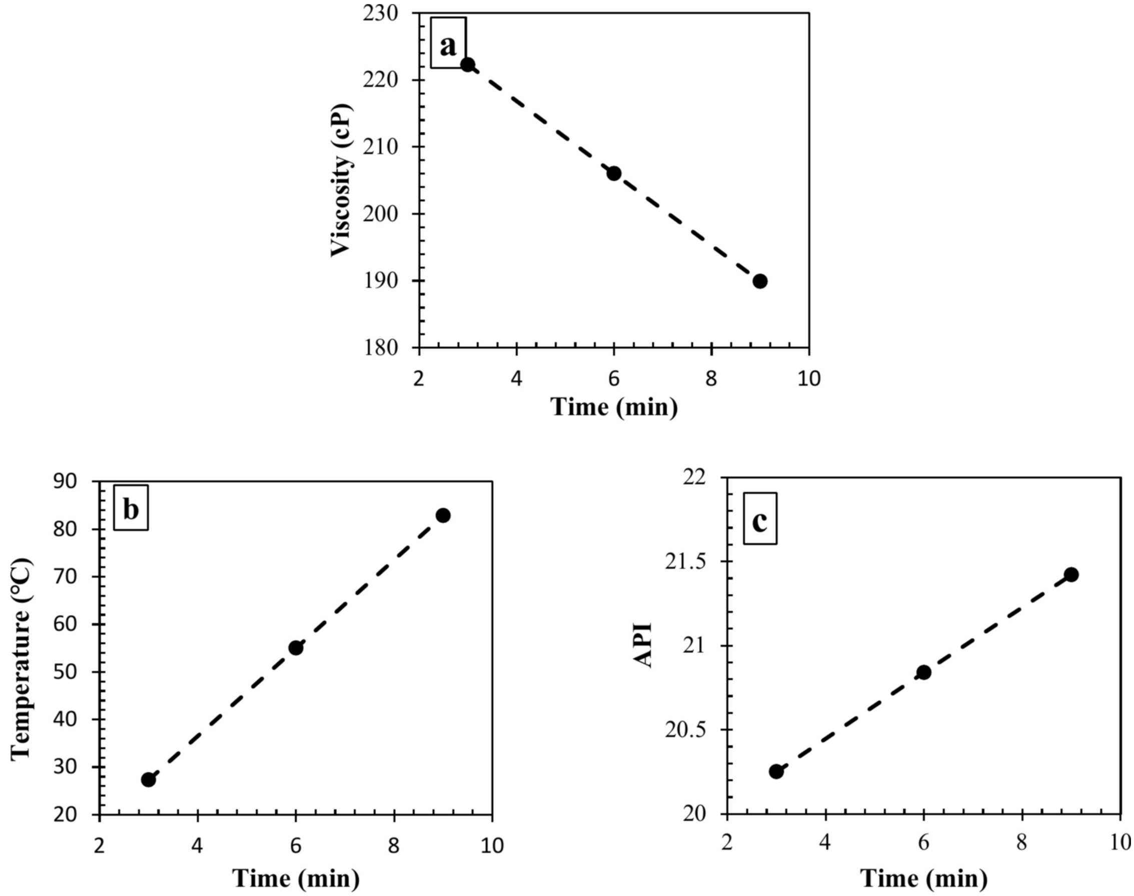

Fig. 10. Effect of duration of MW radiation on a) viscosity, b) temperature and c) API for the Fe_3O_4-NiO nanoparticle in 0.5 wt.% concentration and the 400 W power.

electromagnetic waves. As a result, the temperature of the oil solution containing these nanoparticles increases the most. Also, the highest increase in temperature and the most significant decrease in viscosity are attributed to these hybrid nanoparticles. However, it should be noted that at high nanoparticle concentrations, their absorptive effects on reducing crude oil viscosity and density may diminish and even lead to an increase in crude oil viscosity. Therefore, to use this method optimally, an appropriate concentration for nanoparticles, power and time for MW must be determined.

To assess the simultaneous effect of nanoparticles and MW radiations on the quality of the crude oil, the viscosity and API of the crude oil are measured in optimal conditions. As mentioned earlier, the viscosity of the crude oil was 330 cP. After applying the radiation of the MW in optimal conditions, the viscosity was measured at 192 cP, indicating a 42.6% decrease in viscosity. Furthermore, the API, measured at 16.97 in the initial crude oil conditions, increased to 21.47. The mentioned changes are the direct result of the nanoparticles, acting as catalysts, coupled with the waves breaking the heavy molecules of the oil and prevention of the aggregation of heavier components such as asphaltene. It has been observed that the viscosity reduction achieved with the Fe_3O_4-NiO nanoparticles along with MW is relatively greater than that reported for other nanoparticles in the literature[21,46].

The effect of nanomaterial on asphaltene onset point

So far, the effect of the simultaneous use of nanoparticles and MW on the static properties of crude oil has been investigated. It was found that using magnetic nanoparticles in conjunction with MW improves the properties of the oil, including viscosity and API, potentially breaking down heavy molecules such as asphaltene. In this part of the study, the accuracy of this effect is checked by investigating the asphaltene onset point and the amount of asphaltene. In other words, the inhibitory role of nanoparticles to prevent asphaltene precipitation was investigated. Additionally, to determine the changes in asphaltene, FTIR, SEM, and EDS tests have been performed on crude oil asphaltene and asphaltene of oil solution under optimal conditions.

The strong polarity of asphaltene leads to their self-association and deposition. The adsorption of asphaltene molecules on the surface of nanoparticles causes their stabilization in crude oil. In this section, the effect of bare and synthesized nanoparticles on crude oil is analyzed. Asphaltene adsorbs onto the surface of bare and synthesized nanoparticles, creating an electrostatic equilibrium that leads to an extended period in which the asphaltene molecules remain stable. This happens due to the electrostatic equilibrium between the nanoparticles

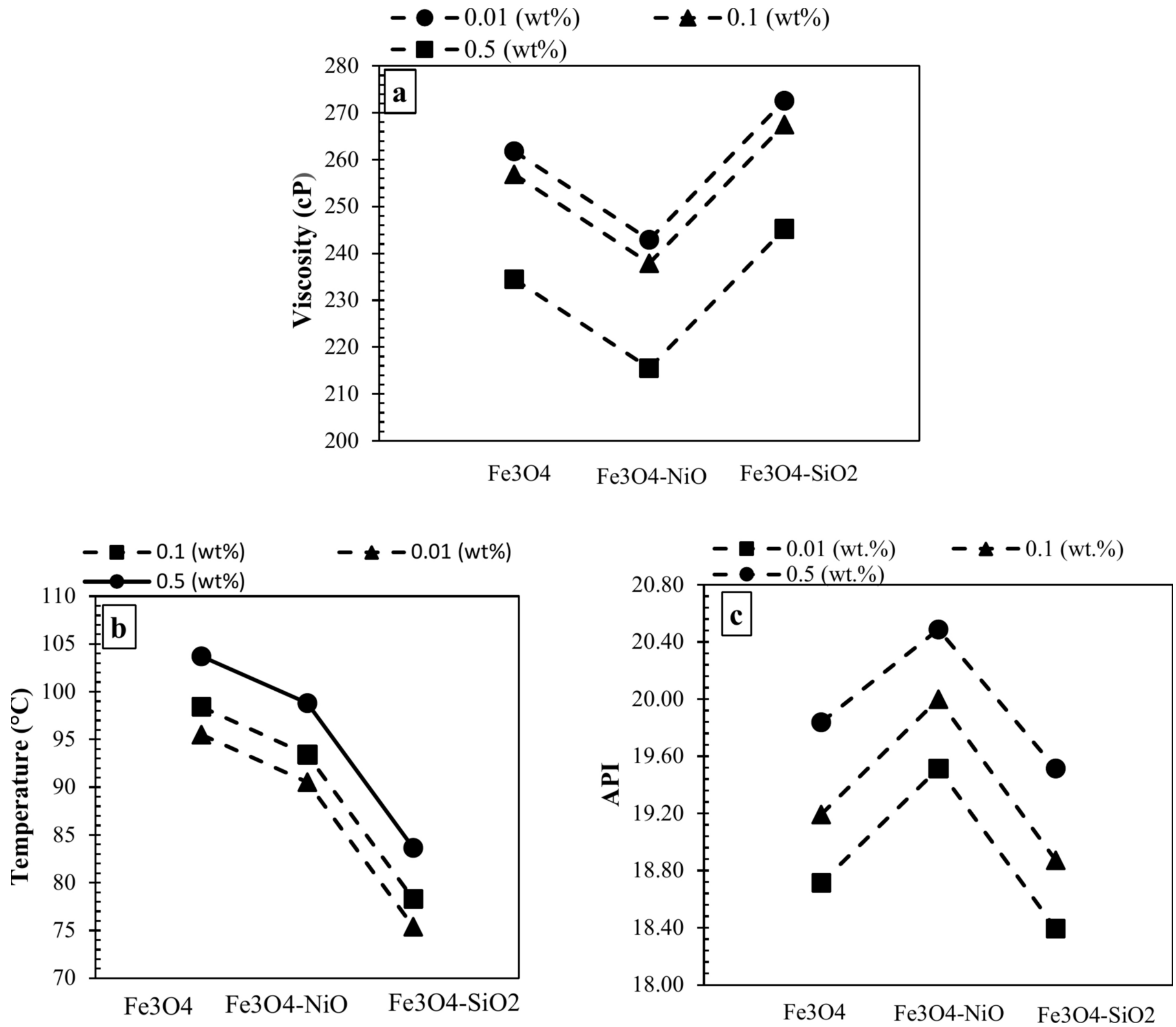

Fig. 11. Interaction between type and concentration of nanoparticles under MW irradiation for a) viscosity, b) temperature and c) API with MW power of 400W and duration of 9 min .

Nanoparticle type	Viscosity (cP)		T (°C)		API	
	Experimental	DOE result	Experimental	DOE result	Experimental	DOE result
Fe_3O_4	208	215	88.2	85.4	20.98	20.81
Fe_3O_4-SiO_2	220	221	69.1	67.9	20.49	20.65
Fe_3O_4-NiO	192	201	83	77.8	21.47	21.31

Table 6. Viscosity, temperature, and density responses for Fe_3O_4, Fe_3O_4-SiO_2, and Fe_3O_4-NiO nanoparticles under MW radiations with optimal conditions.

and asphaltene molecules.. Nanoparticles' surface charge distribution can be altered, enabling them to adsorb asphaltenes and prevent aggregation and deposition in the reservoir. Thus, nanoparticle adsorption effectively inhibits asphaltene deposition.

Figure 12 demonstrates the effect of nanoparticles on the asphaltene onset point. The onset of asphaltene precipitation is indicated by a bump in the viscosity diagram with respect to the volume percentage of n-heptane. For crude oil, the onset of asphaltene is observed at 10 Vol.% n-heptane by volume. This onset is delayed to 12 Vol.% n-heptane for Fe_3O_4 and NiO nanoparticles and to 13 Vol.% n-heptane for SiO_2nanoparticles, which falls within the normal range reported in previous studies of these nanoparticles[38]. SiO_2 nanoparticles have a negative surface charge in oil solutions, primarily due to the deprotonation of silanol (Si–OH) groups on the surface, which is also present on SiO_2 nanoparticles modified with oleic acid. Additionally, the carboxylate group (-COO$^-$

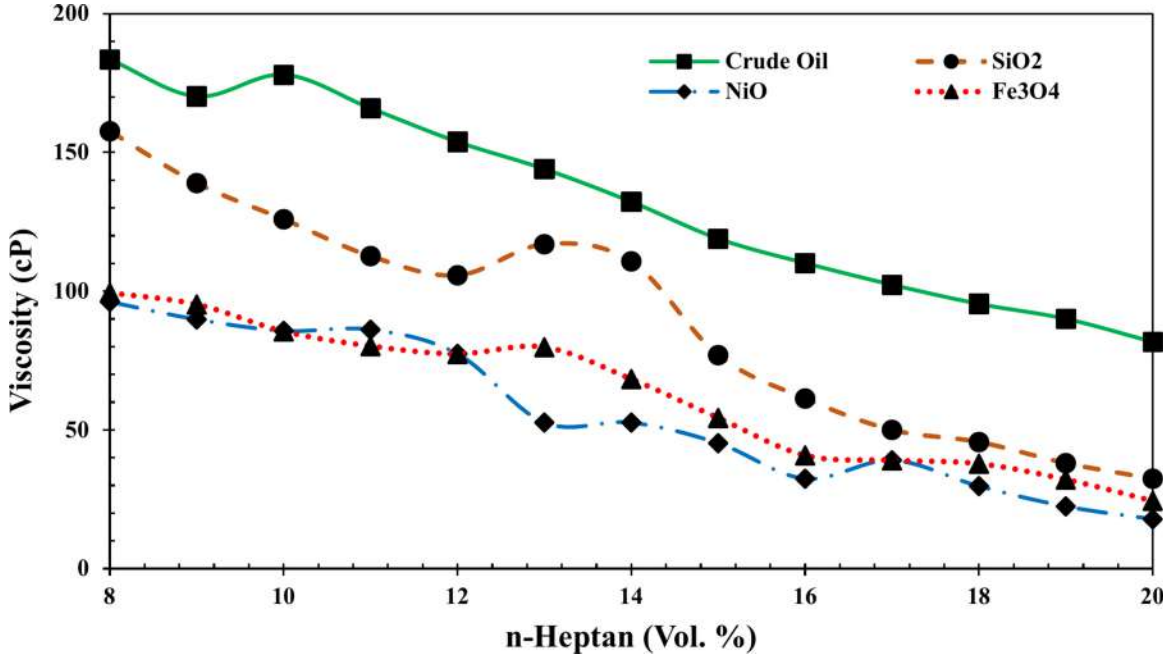

Fig. 12. Onset analysis of asphaltene precipitation for crude oil and crude oil with SiO2, NiO and Fe_3O_4.

) of oleic acid can interact with asphaltene molecules, stabilizing them in the oil. This functional group creating a repulsive force between the asphaltene molecules and the surface-modified SiO_2 with oleic acid.

Simultaneous application of nanoparticles with MW

The analyses of the simultaneous effect of the nanoparticles along with MW radiation are presented in Fig. 13. MW radiation improves the onset of asphaltene precipitation by increasing the temperature and reducing viscosity as discussed in section "Crude oil temperature alteration in presence of nanoparticles and MW", by disrupting the intermolecular forces and bonding between asphaltene molecules, MW causes asphaltene stability and improves asphaltene onset, and preventing their aggregation and deposition. NiO nanoparticle inhibit asphaltene precipitation by absorbing asphaltene molecules, creating electrostatic stabilization, MW energy absorption and increasing the effects of it treatment, and break down asphaltene molecules as chemical catalysts. These mechanisms work together to stabilize asphaltenes when use NiO nanoparticles in crude oil, delaying the onset of asphaltene to 18 Vol.% n-heptane and preventing aggregation and precipitation. Additionally, the application of MW in the presence of Fe_3O_4 nanoparticles enhances the onset of asphaltene point. This enhancement is attributed to the increased temperature and decreased viscosity of crude oil, as discussed in sections "Crude oil temperature alteration in presence of nanoparticles and MW" and "DOE results". In contrast, SiO_2 nanoparticles, lacking electromagnetic properties, do not align in the presence of MW and do not exhibit a significant temperature increase (section "Crude oil temperature alteration in presence of nanoparticles and MW"), resulting in no improvement in their performance in presence of MW.

Onset of asphaltene in optimum points

As discussed earlier, Fe_3O_4, Fe_3O_4-NiO and Fe_3O_4-SiO_2 nanoparticles was synthesis using the co precipitation method. These hybrids were synthesized solely for the purpose of this test. To explain this in a more precise manner, the previous conducted tests in this research, demonstrated that Fe_3O_4 is an excellent wave energy absorber due to its magnetic properties. Furthermore, based on previous studies NiO is a good nano-inhibtor. Consequently, their hybrid should excel in both categories. Based on the same concept the Fe_3O_4-SiO_2 should perform well form both absorption and nano-inhibitor point of view. As is observed after the addition of the Fe_3O_4 and its hybrids (with SiO_2 and NiO) coupled with the instigation caused from the MW radiation, the asphaltene onset is higher compared with the crude oil case (Fig. 14).

As it is known, the onset of asphaltene precipitation after adding three nanoparticles and exposure to MW increased compared to the precipitation point of crude oil asphaltene. This increase in Fe_3O_4-NiO and Fe_3O_4-SiO_2 nanohybrids is more than Fe_3O_4 nanoparticle is due to the property of simultaneous absorption of asphaltene and MW by these nanohybrids. Fe_3O_4 nanoparticles provide asphaltene inhibition due to strong MW interaction, localized heating by creating hotspot, and effective asphaltene adsorption. Also, Fe_3O_4-SiO_2 show moderate asphaltene inhibition, benefiting from Fe_3O_4 properties but limited by SiO_2 lower interaction with MW. The SiO_2 component still aids in adsorption of asphaltene but does not significantly enhance MW effects. The energy absorbed by the absorbent part, i.e. Fe_3O_4, can cause asphaltene absorbed on the other surface of the nano-hybrid to be broken. In this way, the radiated energy causes the absorption of asphaltene molecules and its breakdown. The special increase in the onset of asphaltene precipitation for the Fe_3O_4-NiO nanohybrid,

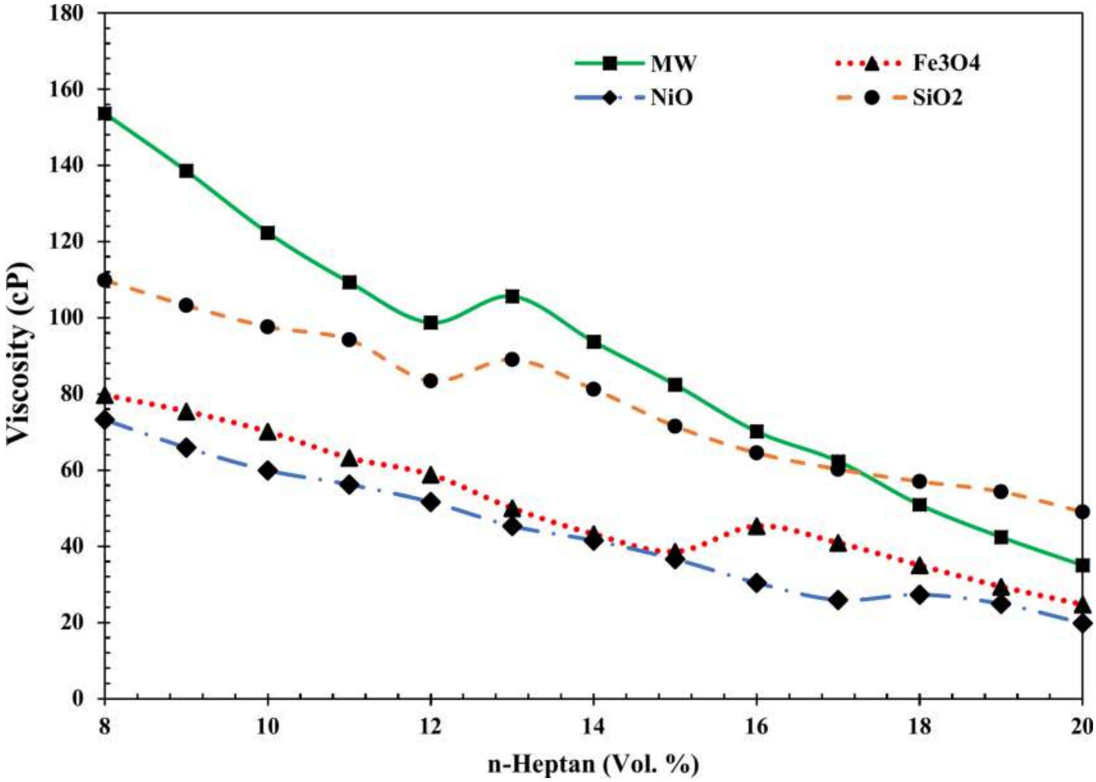

Fig. 13. Onset of asphaltene precipitation for crude oil and crude oil with SiO_2, NiO and Fe_3O_4 nanoparticles along with MW.

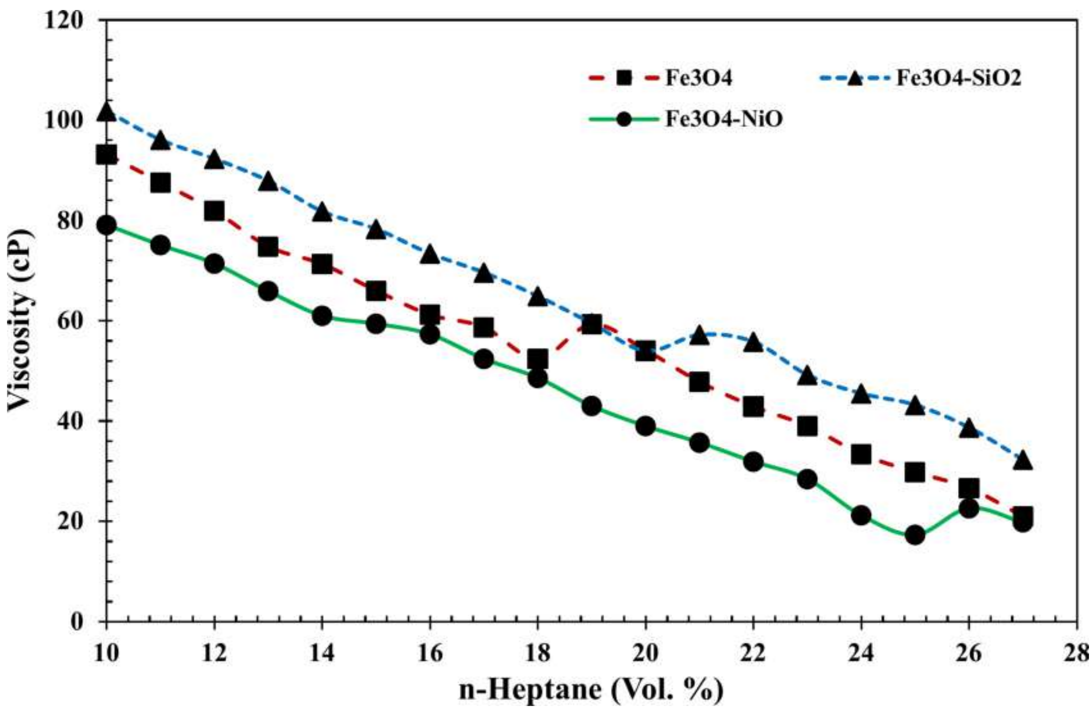

Fig. 14. Onset of asphaltene precipitation for optimum condition for Fe_3O_4, Fe_3O_4-NiO and Fe_3O_4-SiO_2 along with MW.

compared to the Fe_3O_4-SiO_2 nanohybrid, is due to the simultaneous absorption of MW and asphaltene molecules near the NiO nanoparticles. This interaction breaks down asphaltene into lighter components, leading to a more stable electrostatic equilibrium between the new lighter asphaltene molecules and the Fe_3O_4-NiO nanohybrid.

Asphaltene extraction results

Asphaltene play a significant role in absorbing MW waves due to the polar elements in their structure, leading to their molecules orienting towards the electromagnetic field. This alignment creates hot spots where the likelihood of asphaltene and resin presence increases, subsequently breaking down these heavy compounds. Figure 15 illustrates a 9.2% reduction in asphaltene content in oil from MW radiation alone respect to crude oil, with a 22.6% decrease observed under simultaneous MW radiation with Fe_3O_4-NiO nanoparticles in optimized conditions. The asphaltene's absorption on the nanoparticles surface, combined with MW energy absorption, contributes to breaking down heavy molecules into lighter ones, reducing asphaltene content attributed to its stronger effect on polar particles.

Result of characterization of asphaltene structure

To check asphaltene changes under various condition, FTIR, EDS, and SEM tests were performed on asphaltenes of crude oil and optimal conditions. As shown in the Fig. 16, the FTIR results indicate that oil asphaltene undergoes significant changes when exposed to simultaneous MW and nanoparticles under optimal conditions. To analyze these changes, defined coefficients (Sect. "Synthesis, surface modification and characterization of nanoparticles") are used to provide a detailed assessment.

Table 7 displays the defined indexes for each sample, revealing an increase in the aliphatic coefficient in asphaltene under MW radiation compared to crude oil asphaltene. Additionally, the aliphatic to aromatic coefficient ratio in asphaltene is higher under MW irradiation (optimal condition), indicating the breakdown of central aromatic nuclei into aliphatic compounds. The branching coefficient of alkane increasing under MW treatment by affecting aromatic structures and converting them into chain structures. Furthermore, the sulfoxide coefficient in asphaltene decreases. This decrease can be attributed to sulfur's strong absorption of MW, leading to the breaking of sulfoxide bonds by the radiated wave energy.

The peak at 720 ± 10 cm^{-1} is related to the $-CH_2$ rock bonds, indicating the presence of long-chain alkanes. Peaks in the 700–900 cm^{-1} range are directly related to the aromatic bonds of a substance. The spectra of both asphaltene samples exhibit two intense and sharp peaks in this range, with their intensities decreasing upon MW radiation in the presence of Fe_3O_4-NiO nanoparticles. Additionally, the peak observed at 1030 cm^{-1} corresponds to the sulfoxide (S = O) bond, demonstrating a significant reduction under optimal conditions. The absorbance peak decreased from 31.9% to 4.75%, which corresponds to a reduction in the sulfoxide index from 0.215 to 0.027.

The SEM image in Fig. 17 displays the extracted asphaltene structure, highlighting differences compared to crude oil asphaltene under MW and using Fe_3O_4-NiO optimal conditions. Voids observed on the asphaltene surface at these points are attributed Fe_3O_4-NiO nano-hybrids absorbing MW energy and asphaltene particles simultaneously, leading to direct effects on the asphaltene structure and the formation of pores (red circles). As is well known, separating these particles from asphaltene reduces its molecular weight. As a result, the stability of asphaltene in crude oil increases. Additionally, the pores created on asphaltene structure can help keep it suspended in the oil solution. These factors, combined with the inhibitory role of Fe_3O_4-NiO nanoparticles, contribute to improvement of asphaltene onset as reported in Fig. 14.

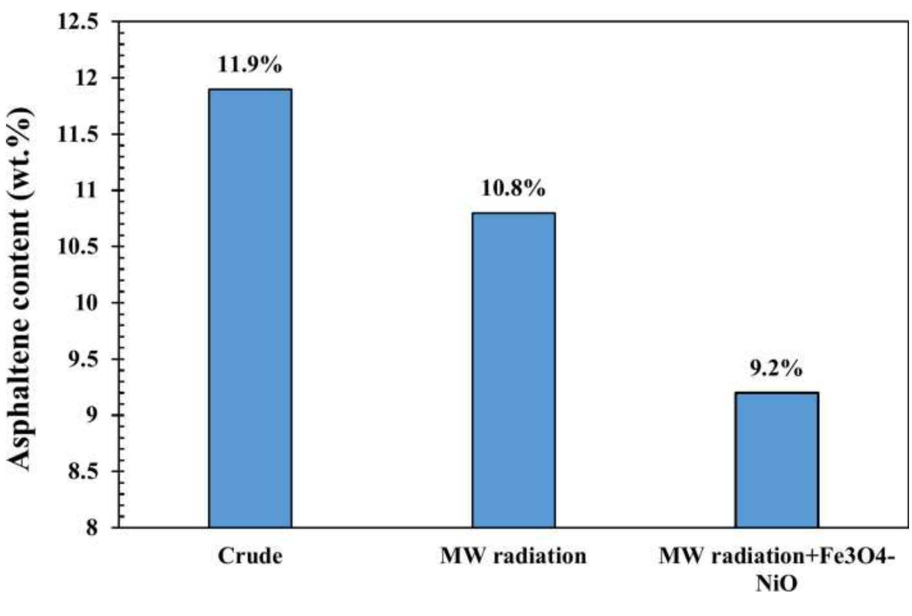

Fig. 15. Asphaltene content of oil under various condition.

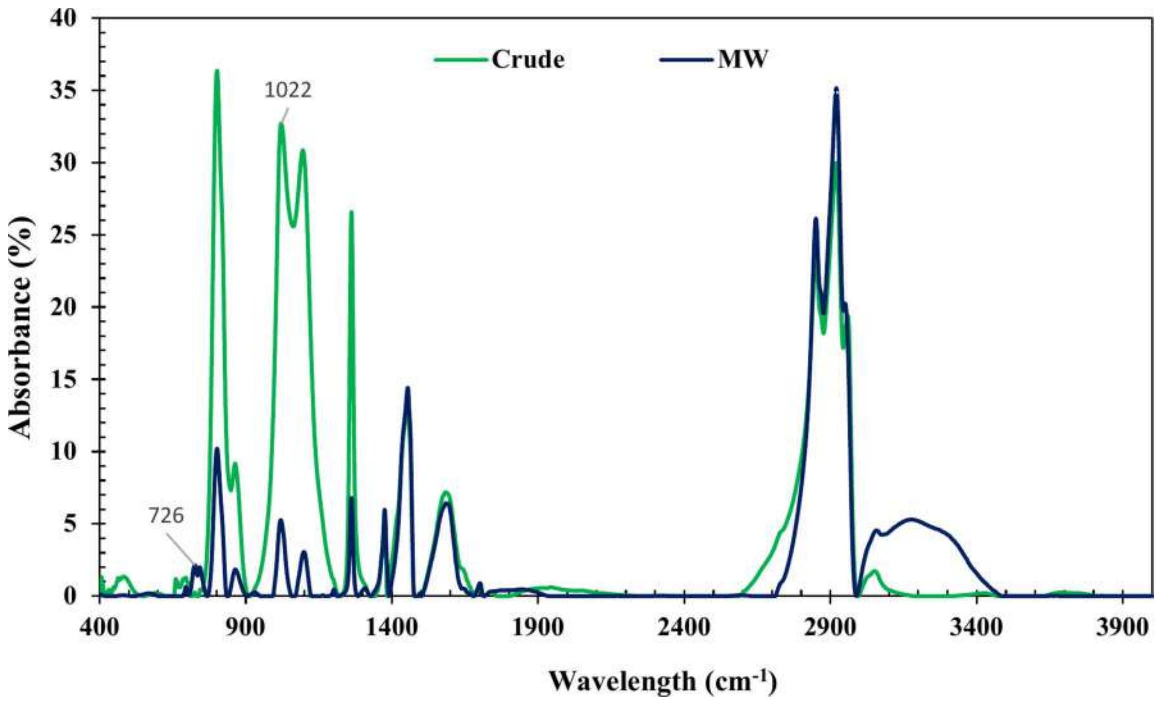

Fig. 16. FTIR of Asphaltene extracted from crude oil and oil under optimal conditions.

Index	Crude asphaltene	Asphaltene of optimum point
Aromatic	0.063	0.08
Aliphatic	0.074	0.116
Sulfoxide	0.215	0.027
Alkane chain Index	0.145	0.161
Aliphatic to Aromatic ratio	1.153	1.455

Table 7. Indexes of asphaltene in crude oil and oil under optimal conditions.

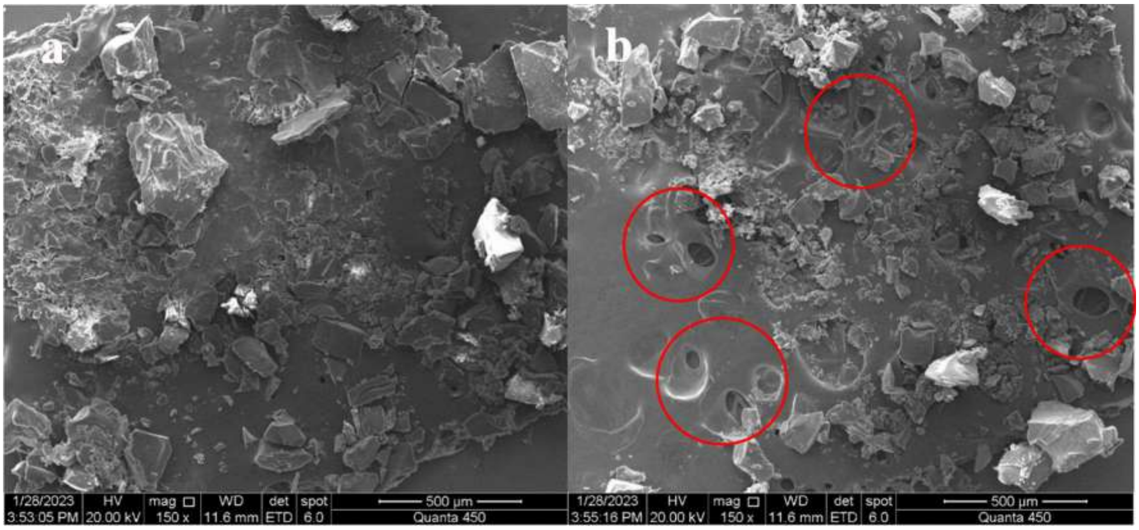

Fig. 17. SEM of the crude oil's Asphaltene a) before and b) after treatment (optimal conditions).

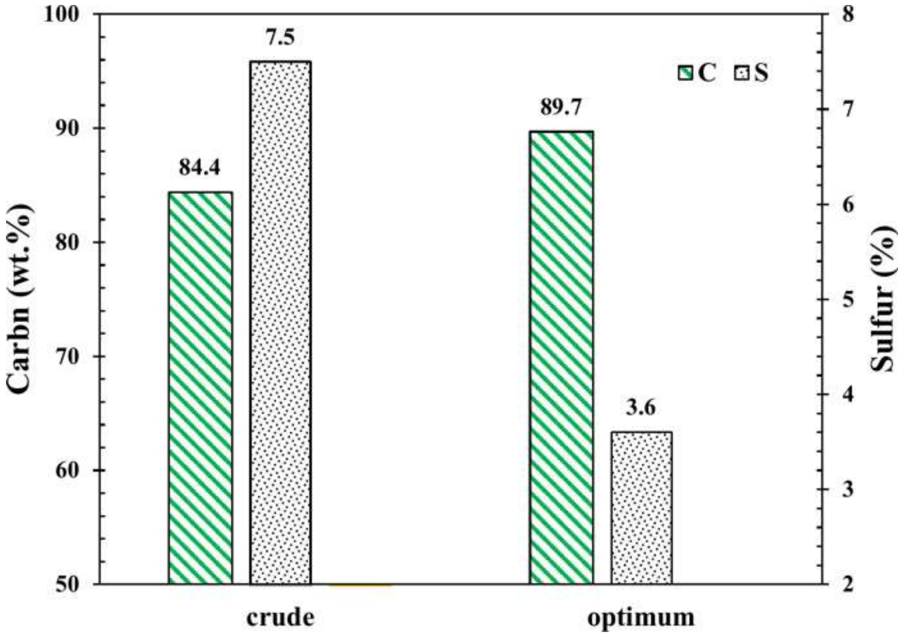

Fig. 18. Carbon and Sulfur wt.% in EDS of Asphaltene extracted from crude oil and oil under optimal conditions.

Figure 18illustrates EDS test results for carbon and sulfur of asphaltene under optimal MW conditions. Carbon content increased by 3.6% through the removal of polar compounds like sulfur, nitrogen, and oxygen due to MW energy absorption by this polar element. Under optimal conditions, sulfur decreased by 52% which approve sulfoxide reduction in FTIR results, more significant than what has been reported so far in th literature[3]. Carbon increased by 6.27% respect to crude oil, indicative of lesser impact on polar elements. This reduction in sulfur and increase in carbon signify improved oil quality, with sulfur transforming into hydrogen sulfide and sulfur dioxide upon wave energy absorption. Reducing the amount of polar asphaltene compounds causes asphaltene stability and decreases the amount of asphaltene deposition.

Conclusion

In this study, the combined effect of nanoparticles and MW was investigated as potential means to improve oil recovery processes. The static oil properties and asphaltene stabilization (through asphaltene onset point) were chosen as realistic representetives for demonstrating the improvement results. The research successfully illustrated that the right combination of magnetic based hybrids combined with MW substantially improve heavy oil quality for extraction, showing promise for large scale implementations.

- The experiments demonstrated that Fe_3O_4-NiO is the most effective at absorbing irradiated energy and generating hot zones, raising the temperature by an average of 225%, which is a 165% improvement over crude oil without nanoparticles. The efficiency of Fe_3O_4-NiO increases with higher irradiated energy. However, excessive temperature increases may lead to the evaporation of lighter oil components, causing a significant rise in oil viscosity.
- The optimimum condtions for the best quality improvement was 9 min radiation time, 400 watts power, and 0.5 wt. % concentration. Also, it is more efficient for the same amount of energy to be emmited for a longer period. In other words, less power and more irradiation time compared to the opposite scenario.
- Although without MW SiO_2 is the most efficient for improving the onset at 13% heptane volume compared to 12% for Fe_3O_4 and NiO, the MW, radiation signficantly improves the results for latter improving them to 16% and 18% respectively. Ultimately, the hybrid form of Fe_3O_4 and NiO combined with radiation displays an even larger improvement, jumping to 26% heptane volume as its onset point.
- The asphaltene extraction results show that the asphaltene content decreased by 22.6% . Additionally, the SEM images illustrate the formation of porous structures in the asphaltenes which is an indication of their stability. This result is further validated by FTIR and EDS, showing a sharp 52% relative decrease in sulfur components which are attributed to the polarity of asphaltene.

Although the Fe_3O_4-NiO results show a lot of promise, it is important to point out that reservoir conditions may substantially impact the properties of the nanoparticles. Future research could focus on investigating the effects of nanoparticles in reservoir pressure and temperature, the influence of salinity on nanoparticle performance, the interactions between nanoparticles and reservoir rock, and the synthesis of nanoparticles at an industrial scale.

Data availability

All data generated or analysed during this study are included in this article. Email for contact: ajafari@modares.ac.ir.

Received: 22 September 2024; Accepted: 12 February 2025
Published online: 17 February 2025

References

1. Hasanvand, M. Z. & Golparvar, A. A critical review of improved oil recovery by electromagnetic heating. *Pet. Sci. & Technol.* **32**(6), 631–637. https://doi.org/10.1080/10916466.2011.592896 (2014).
2. Bera, A. & Babadagli, T. Status of electromagnetic heating for enhanced heavy oil/bitumen recovery and future prospects: A review. *Appl. Energy* **151**, 206–226. https://doi.org/10.1016/j.apenergy.2015.04.031 (2015).
3. Gharibshahi, R., Omidkhah, M. & Jafari, A. Parametric optimization of in-situ heavy oil upgrading using simultaneous microwave radiation and magnetic nanohybrids via taguchi approach. *SSRN Electron. J.* https://doi.org/10.2139/ssrn.4017218 (2022).
4. Shamsi Armandi, H., Jafari, A., Gharibshahi, R. & Omidkhah, M. Application of electromagnetic waves and their effects on 'rock-fluid' and 'fluid-fluid' interactions in enhanced oil recovery. *Sci. Propagative J. Oil Gas Explor. Prod.* **171**, 40–48 (2019).
5. Morte, M., Dean, J., Kitajima, H. & Hascakir, B. Increasing the penetration depth of microwave radiation using acoustic stress to trigger piezoelectricity. *Energy & Fuels* **33**(7), 6327–6334. https://doi.org/10.1021/acs.energyfuels.9b01150 (2019).
6. Farshadfar, H., Shamsi Armandi, H., Gharibshahi, R. & Jafari, A. Simultaneous electromagnetic radiation and nanofluid injection and their interactions in EOR operations: A comprehensive review. *J. Magn. Magn. Mater.* **580**, 170863. https://doi.org/10.1016/j.jmmm.2023.170863 (2023).
7. Torkaman, P., Karimzadeh, R. & Jafari, A. Synthesis of Fe3O4-Mn2O3 and Fe3O4-Graphene oxide hybrid nanocatalyst and their effects on the electromagnetic properties and their performance on heavy hydrocarbons upgrading. *J. Anal. Appl. Pyrolysis* **179**, 106467. https://doi.org/10.1016/j.jaap.2024.106467 (2024).
8. Gu, Z., Lu, T., Li, Z. & Xu, Z. Experimental investigation on the SiO2 nanoparticle foam system characteristics and its advantages in the heavy oil reservoir development. *J. Pet. Sci. Eng.* **214**, 110438. https://doi.org/10.1016/j.petrol.2022.110438 (2022).
9. Shi, Y., Wang, X. & Mohanty, K. Effect of a nanoparticle on wettability alteration and wettability retainment of carbonate reservoirs. *J. Pet. Sci. Eng.* **215**, 110684. https://doi.org/10.1016/j.petrol.2022.110684 (2022).
10. Namdar, H., Manteghian, M., Jafari, A. & Riazi, M. Analysis and optimization of binary interactions in the aquathermolysis of heavy oil catalyzed by trimetallic nanoparticles. *J. Anal. Appl. Pyrolysis* **178**, 106402. https://doi.org/10.1016/j.jaap.2024.106402 (2024).
11. Gharibshahi, R., Asadzadeh, N. & Jafari, A. Toward understanding the effect of electromagnetic radiation on in situ heavy oil upgrading and recovery: background and advancements. In *Innovations in Enhanced and Improved Oil Recovery - New Advances* (ed. Zoveidavianpoor, M.) 161–183 (IntechOpen, Rijeka, 2023). https://doi.org/10.5772/intechopen.1002809
12. Sun, X., Zhang, Y., Chen, G. & Gai, Z. Application of nanoparticles in enhanced oil recovery: A critical review of recent progress. *Energies* **10**, 3. https://doi.org/10.3390/en10030345 (2017).
13. Millemann, R. E., Haynes, R. J., Boggs, T. A. & Hildebrand, S. G. Enhanced oil recovery: Environmental issues and state regulatory programs. *Environ. Int.* **7**(3), 165–177. https://doi.org/10.1016/0160-4120(82)90103-9 (1982).
14. Yang, S., Yan, C., Cai, J., Pan, Y. & Han, Q. Research progress in nanoparticle inhibitors for crude oil asphaltene deposition. *Molecules* **29**, 5. https://doi.org/10.3390/molecules29051135 (2024).
15. Agista, M. N., Guo, K. & Yu, Z. A state-of-the-art review of nanoparticles application in petroleum with a focus on enhanced oil recovery. *Appl. Sci.* **8**, 6. https://doi.org/10.3390/app8060871 (2018).
16. Fopa, R. D., Bianco, C., Archilha, N. L., Moreira, A. C. & Pak, T. A pore-scale investigation of the effect of nanoparticle injection on properties of sandy porous media. *J. Contam. Hydrol.* **253**, 104126. https://doi.org/10.1016/j.jconhyd.2022.104126 (2023).
17. Hosny, R. et al. Nanotechnology impact on chemical-enhanced oil recovery: A review and bibliometric analysis of recent developments. *ACS Omega* **8**(49), 46325–46345. https://doi.org/10.1021/acsomega.3c06206 (2023).
18. Hasani, M. & Jafari, A. Electromagnetic field's effect on enhanced oil recovery using magnetic nanoparticles: Microfluidic experimental approach. *Fuel* **307**, 121718. https://doi.org/10.1016/j.fuel.2021.121718 (2022).
19. Sabzi dizajyekanJafariHasaniVafaei-SeftiFakhroueianBaghbansalehi, B. A. M. M. Z. M. Surface modification of synthesized Fe3O4 super-paramagnetic nanoparticles and performance investigation in gelation parameters enhancement: application in enhanced oil recovery. *Appl. Nanosci.* **10**(3), 955–969. https://doi.org/10.1007/s13204-019-01187-y (2020).
20. Gharibshahi, R., Omidkhah, M., Jafari, A. & Fakhroueian, Z. Hybridization of superparamagnetic Fe3O4 nanoparticles with MWCNTs and effect of surface modification on electromagnetic heating process efficiency: A microfluidics enhanced oil recovery study. *Fuel* **282**(November), 2020. https://doi.org/10.1016/j.fuel.2020.118603 (2019).
21. Torkaman, P., Karimzadeh, R. & Jafari, A. Assessment of the synthesis method of Fe3O4 nanocatalysts and its effectiveness in viscosity reduction and heavy oil upgrading. *Sci. Rep.* **13**(1), 1–14. https://doi.org/10.1038/s41598-023-41441-6 (2023).
22. A. M. S. Ragab and A. E. Hannora, A comparative investigation of nano particle effects for improved oil recovery - experimental work *Soc. Pet. Eng. - SPE Kuwait Oil Gas Show Conf.* 2015 https://doi.org/10.2118/175395-ms.
23. Yahya, N. et al. Improved oil recovery by high magnetic flux density subjected to iron oxide nanofluids. *J. Nano Res.* **26**, 89–99. https://doi.org/10.4028/www.scientific.net/JNanoR.26.89 (2014).
24. Adil, M., Zaid, H. M., Chuan, L. K. & Latiff, N. R. A. Influence of electromagnetic waves on viscosity and electrorheology of dielectric nanofluids-scale-based approach. *J. Teknol.* **78**(6–4), 49–54. https://doi.org/10.11113/jt.v78.8974 (2016).
25. Ali, H. et al. Absorption of electromagnetic waves in sandstone saturated with brine and nanofluids for application in enhanced oil recovery. *J. Taibah Univ. Med. Sci.* **14**(1), 217–226. https://doi.org/10.1080/16583655.2020.1718467 (2020).
26. Nasri, Z. Upgrading vacuum distillation residue of oil refinery using microwave irradiation. *Chem. Eng. Process. - Process Intensif.* **146**, 107675. https://doi.org/10.1016/j.cep.2019.107675 (2019).
27. J. Taheri-Shakib, A. Shekarifard, H. Naderi, S. A. Hosseini, 2017 Effect of microwave irradiation on wax and asphaltene content of heavy crude oil *79th EAGE Conf. Exhib. 2017* 12–15 https://doi.org/10.3997/2214-4609.201700699.
28. Taheri-shakib, J., Shekarifard, A. & Naderi, H. The experimental investigation of effect of microwave and ultrasonic waves on the key characteristics of heavy crude oil. *J. Anal. Appl. Pyrolysis* https://doi.org/10.1016/j.jaap.2017.10.021 (2017).
29. Gharibshahi, R., Omidkhah, M., Jafari, A. & Fakhroueian, Z. Experimental investigation of nanofluid injection assisted microwave radiation for enhanced heavy oil recovery in a micromodel system. *Korean J. Chem. Eng.* **39**(3), 562–575. https://doi.org/10.1007/s11814-021-0961-7 (2022).
30. Campen, S., Moorhouse, S. J. & Wong, J. S. S. Mechanism of an asphaltene inhibitor in different depositing environments: Influence of colloid stability. *J. Pet. Sci. Eng.* **184**(May), 2020. https://doi.org/10.1016/j.petrol.2019.106502 (2019).
31. Hashemi, R., Nassar, N. N. & Pereira Almao, P. Nanoparticle technology for heavy oil in-situ upgrading and recovery enhancement: Opportunities and challenges. *Appl. Energy* **133**, 374–387. https://doi.org/10.1016/j.apenergy.2014.07.069 (2014).
32. Jafari, A., Farjami Shayesteh, S., Salouti, M. & Boustani, K. Dependence of structural phase transition and lattice strain of Fe3O4 nanoparticles on calcination temperature. *Indian J. Phys.* **89**(6), 551–560. https://doi.org/10.1007/s12648-014-0627-y (2015).

33. Zhao, L. et al. The effect of aging time and calcination temperature on the magnetic properties of α-Fe/Fe3O4 composite. *J. Magn. Magn. Mater.* **301**(2), 287–291. https://doi.org/10.1016/j.jmmm.2005.07.029 (2006).
34. Li, Z. & Zhu, Y. Surface-modification of SiO 2 nanoparticles with oleic acid. *Appl. Surf. Sci.* **211**(1–4), 315–320. https://doi.org/10.1016/S0169-4332(03)00259-9 (2003).
35. Khairnar, S. D. & Shrivastava, V. S. Facile synthesis of nickel oxide nanoparticles for the degradation of Methylene blue and Rhodamine B dye: a comparative study. *J. Taibah Univ. Sci.* **13**(1), 1108–1118. https://doi.org/10.1080/16583655.2019.1686248 (2019).
36. Soleymanzadeh, A., Yousefi, M., Kord, S. & Mohammadzadeh, O. A review on methods of determining onset of asphaltene precipitation. *J. Pet. Explor. Prod. Technol.* **9**(2), 1375–1396. https://doi.org/10.1007/s13202-018-0533-5 (2019).
37. Taherian, Z., Dehaghani, A., Ayatollahi, S. & Kharrat, R. A New Insight to the Assessment of Asphaltene Characterization by Using Fortier Transformed Infrared Spectroscopy. *J. Pet. Sci. Eng.* **205**, 108824. https://doi.org/10.1016/j.petrol.2021.108824 (2021).
38. Shadervan, A., Jafari, A., Teimouri, A., Gharibshahi, R. & Dehaghani, A. H. S. Mechanistic understanding of asphaltene precipitation and oil recovery enhancement using SiO2 and CaCO3 nano-inhibitors. *Sci. Rep.* **14**(1), 1–20. https://doi.org/10.1038/s41598-024-65995-1 (2024).
39. Gong, M., Yao, Z., Xiong, Z., Yang, J. & Hong, J. Investigation on the influences of moisture on asphalts' micro properties by using atomic force microscopy and Fourier transform infrared spectroscopy. *Constr. Build. Mater.* **183**, 171–179. https://doi.org/10.1016/j.conbuildmat.2018.05.189 (2018).
40. Zojaji, I., Esfandiarian, A. & Taheri-Shakib, J. Toward molecular characterization of asphaltene from different origins under different conditions by means of FT-IR spectroscopy. *Adv. Colloid Interface Sci.* **289**, 102314. https://doi.org/10.1016/j.cis.2020.102314 (2021).
41. Permanyer, A., Rebufa, C. & Kister, J. Reservoir compartmentalization assessment by using FTIR spectroscopy. *J. Pet. Sci. Eng.* **58**(3–4), 464–471. https://doi.org/10.1016/j.petrol.2005.09.009 (2007).
42. Yan, F., Jiang, J., Chen, X., Tian, S. & Li, K. Synthesis and characterization of silica nanoparticles preparing by low-temperature vapor-phase hydrolysis of SiCl4. *Ind. Eng. Chem. Res.* **53**(30), 11884–11890. https://doi.org/10.1021/ie501759w (2014).
43. Panwar, K., Jassal, M. & Agrawal, A. K. In situ synthesis of Ag-SiO2Janus particles with epoxy functionality for textile applications. *Particuology* **19**, 107–112. https://doi.org/10.1016/j.partic.2014.06.007 (2015).
44. Shang, H. et al. Effect of microwave irradiation on the viscosity of crude oil: A view at the molecular level. *Fuel Process. Technol.* **170**, 44–52. https://doi.org/10.1016/j.fuproc.2017.10.021 (2018).
45. Hasani, M. & Jafari, A. Electromagnetic field's effect on enhanced oil recovery using magnetic nanoparticles: Microfluidic experimental approach. *Fuel* **307**, 121718. https://doi.org/10.1016/j.fuel.2021.121718 (2022).
46. Shamsi Armandi, H., Jafari, A. & Gharibshahi, R. Nanoparticles assisted microwave radiation: Fluid-rock interactions in oil reservoirs. *Pet. Sci.* **18**(6), 1797–1812. https://doi.org/10.1016/j.petsci.2021.09.002 (2021).

Author contributions

Hamidreza Farshadfar: Conceptualization, Data curation, Investigation, Methodology, Validation, Writing—original draft. Reza Gharibshahi: Methodology, Data curation, Validation, Visualization, Writing—review and Editing. Arezou Jafari: Supervision, Funding acquisition, Resources. Sharif Shoushtari: Writing—review and Editing.

Declarations

Competing interests

The authors declare no competing interests.

Additional information

Correspondence and requests for materials should be addressed to A.J.

Reprints and permissions information is available at www.nature.com/reprints.

Publisher's note Springer Nature remains neutral with regard to jurisdictional claims in published maps and institutional affiliations.